Nonannihilation Dynamics of Solutions Arising in Reaction-Diffusion Systems

(反応-拡散系に現れる解の
衝突非消滅ダイナミクス)

長山 雅晴

Nonannihilation Dynamics of Solutions Arising in Reaction-Diffusion Systems
(反応ー拡散系に現れる解の衝突非消滅ダイナミクス)

長山 雅晴

Acknowledgments

I profoundly appreciate Professor Masayasu Mimura, University of Tokyo, for his continual instruction, impressible encouragement and critical reading of the manuscript. This thesis is based on the joint works with him. I might not be what I am without his kind thoughtfulness.

I would like to thank Profrssor Takao Ohta, Ochanomizu University, for useful discussions. Section 3 is based on the joint works with him.

I would like to thank Mr. Ryo Ikota and Mr. Marianito R. Rodrigo for their useful suggestions.

This work was supported by a JSPS Research Fellowships for Young Scientists.

Finally, I would like to thank Ayako, My wife for her warm encouragement.

1 Introduction

Spatio-temporal patterns arising in chemical reactions in diffusive media, population dynamics in ecology, action potentials of nerve fibers, cell-differentiation in developmental biology, combustion, solidification and other pattern dynamics of nature have been mathematically investigated by using reaction-diffusion(RD) systems. Among these patterns, it has been well known that travelling pulses on electrical activity in nerve fibers [13] or expanding rings of Belousov-Zhabotinsky(BZ) reaction [22] in experiments. One typical feature of these patterns is annihilation property as in Figure 1.1. This has been theoretically investigated by using mono-stable excitable RD systems. A simple but suggestive system is described by

$$\begin{cases} \dfrac{\partial u}{\partial t} = \Delta u + \dfrac{1}{\varepsilon} f(u,v), \\ \\ \dfrac{\partial v}{\partial t} = d\Delta v + g(u,v), \end{cases} \qquad t > 0, \quad x \in \boldsymbol{R}^n, \tag{1.1}$$

where $u(t,x)$ and $v(t,x)$ are the concentrations of chemicals or the densities of biological species at time t and position x in $\boldsymbol{R}^n$. These two species are respectively called an activator and its inhibitor in biology or a propagator and its controller in chemistry. The constant d is the ratio of the diffusion rates of u and v and ε is the time constant between the dynamics of u and v. In almost all applications, $f = 0$ takes an S-shape nonlinearity and $g = 0$ is monotone increasing, which intersect at one point in the (u,v)-plane. The first example is that f and g have FitzHugh-Nagumo(FHN) type nonlinearities used in modeling action potentials in nerve fibers [13]

$$f(u,v) = u(u-a)(1-u) - v, \quad g(u,v) = u - \gamma v \tag{1.2}$$

where $0 < a < 1/2$ and $\gamma > 0$ are both constant. The constant γ is required to satisfy that $f = 0$ and $g = 0$ have only one intersection point at the origin $P = (0,0)$ (Figure 1.2). The second is that f and g have Oregonator nonlinearities used in modeling the BZ reaction

[21]

$$f(u,v) = u(1-u) - \alpha v \frac{u-q}{u+q}, \quad g(u,v) = u - v \tag{1.3}$$

where α and q are positive constant, which are required to satisfy that $f = 0$ and $g = 0$ have only one intersection point at P (Figure 1.3).

In order to explain the property of excitability, we consider the diffusionless system of (1.1) with (1.2)

$$\begin{cases} \dfrac{\partial u}{\partial t} = \dfrac{1}{\varepsilon} f(u,v), \\ \qquad\qquad\qquad t > 0, \\ \dfrac{\partial v}{\partial t} = g(u,v), \end{cases} \tag{1.4}$$

which possesses uniquely the globally stable critical point P. In particular, since ε is small, trajectories of the system possesses fast and slow motions in the (u,v)-phase plane: when the initial point $(u,v)(0)$ is near P, then the trajectory directly decays to P, while when it is suitably far from P, it results in a long excursion and then comes back to P (Figure 1.4). Because of this property, (1.4) is called an *excitable system* with only one critical point and the corresponding RD system (1.1) is called an *excitable RD system* with one critical point.

We first note that P is the trivial solution of excitable RD system (1.1), (1.2) and is locally stable for any d. However, when d is not large, a suitably large point perturbation given to the constant state P evolves into an expanding ring, which has the following properties:

(P-1) An expanding ring is stable under small perturbations [20].

(P-2) When two expanding rings collide, they annihilate each other (Figure 1.5).

These properties are also clearly observed in the BZ reaction. From experimental observations and numerical simulations of mathematical models of excitable RD systems with

only one critical point, it has been believed for a long time that stable travelling pulses arising in any 2-component system should satisfy such annihilation property, if they exist.

Recently, it has been shown in some other types of excitable RD systems that when two travelling pulses approach, they do not necessarily annihilate but repel each other. For example, Petrov *et al* [18] have shown that two travelling pulses repel each other in the cubic autocatalytic RD model with three critical points where one is stable, while the other points are unstable. Krisher and Mikhailov [9], Kawaguchi and Mimura [8] have considered (1.1) with global inhibitory coupling term and shown that two travelling pulses and spots exhibit elastic-like collision. Pearson [17] has reported that there occurs nonannihilation of propagating fronts and moreover, there appear a variety of complex spatio-temporal patterns in 2-dimensions in the Gray-Scott model [2].

From the above results, we find that within the class of excitable RD systems, some systems exhibit annihilation while some do not. Hence, we would like to investigate which types of nonlinearities produce annihilation or nonannihilation. Thus, we concentrate our attention to the study of spatio-temporal patterns arising in excitable RD systems which satisfy

(A-1) $f(u,v) = 0$ takes cubic like nonlinearity, $g(u,v) = 0$ is a monotone function and these intersect at only one point such that the system (1.4) possesses excitability for small ε.

(A-2) (1.1) has a stable travelling pulse solution.

We now address the following question:

Do travelling pulses of (1.1) *exhibit nonannihilation phenomenon under the assumption (A-1) and (A-2) ?*

We already knew that the FHN equations and the Oregonator model do not possess such phenomenon.

Here, we take f and g in (1.1) as the following first order exothermic nonlinearities.

$$f(u,v) = -au + k(u)v, \quad g(u,v) = h(v_c - v) - k(u)v \tag{1.5}$$

with $k(u) = \exp(u/(1+u/c))$, where the variables $u(t,x)$ and $v(t,x)$ of (1.1) respectively correspond to the temperature and the concentration of chemical reactant at time t and position x, parameters a, h, v_c and c are all positive constants [12]. The explanation of (1.1), (1.5) is stated in the next section.

Let us first demonstrate some numerical simulations where a, h, v_c and c are suitably fixed to satisfy (A-1), as in Figure 1.6. We fix ε take small but not sufficiently small. If d is smaller than unity, there is a stable travelling pulse which possesses the annihilation property. In fact, two travelling pulses in 1-dimension and three expanding rings in 2-dimensions annihilate, when they collide (Figures 1.7 and 1.8). On the other hand, if d is larger than unity, there is still a stable travelling pulse which moves very slowly. When two travelling pulses approach, they don't annihilate but repel each other(Figure 1.9). Three expanding rings are broken up into a complex pattern, as in Figure 1.10, in which we can observe the following four features:

(E-1) annihilation of two expanding rings, if the size is small;

(E-2) extinction before collision of two expanding rings, if the size is intermediate;

(E-3) repulsion of two expanding rings, if the size is large;

(E-4) destabilization of planar travelling pulse.

(E-2) and (E-3) suggest that the 2-component RD system with (1.5) exhibits nonannihilation property of travelling pulses and expanding rings, even if the system satisfies (A-1) and (A-2).

As a first step in the understanding of such complex patterns, the following problem naturally arises:

(Pr-1) What is the mechanism behind this nonannihilation phenomenon ?

For this problem, Ohta, Kiyose and Mimura [16] have shown in a similar type of (1.1) with conservation of the total value of u and v which was proposed by Kawaguchi-Mimura model that if two travelling pulses approach each other very slowly then they repel like elastic objects. They emphasized that the conservation property is important to exhibit repulsion of travelling pulses. However, we have numerically shown that excitable RD systems, which satisfy (A-1) and (A-1), have the nonannihilation property, even if they do not have the conservation property.

Under the above situation, the aim of this paper is to make clear problem (Pr-1) for the excitable RD system (1.1). The content of this paper is organized as follows:

Section 2 : In §2.1, we introduce the first order exothermic RD system in the framework of excitable RD systems with one critical point. In §2.2, in order to study the property of travelling pulses, we numerically draw the existence-region of stable travelling pulse solutions when d and ε are globally varied. We find out the very slowly travelling pulses. In order to understand why the very slowly travelling pulses exist, we numerically draw the global structure of standing pulse solutions and bifurcation from standing ones. We find that travelling pulses primary and super-critically bifurcated from the standing ones. In §2.3, we consider the interaction of two travelling pulses which approach each other. We numerically demonstrate that they reflect each other when the velocity is very slow. In order to conjecture that very slowly travelling pulses possess the nonannihilation property, we also treat the Gray-Scott model in the framework of excitable RD systems and show that it also exhibits nonannihilation property of very slowly travelling pulses.
This section is essentially based on result obtained in [10].

Section 3 : In §3.1, in order to analytically show the conjecture stated in §2.3, we introduce the bistable FHN system. In §3.2, to discuss the repulsive interaction of two

travelling pulses, we define the position of travelling pulses as the interface of the limit as $\varepsilon \downarrow 0$ and we derive the limiting system from the bistable FHN system. In §3.3, in order to confirm that the limiting system of the bistable FHN has the nonannihilation property, we consider an interface-interface interaction problem. In §3.4, in order to treat the reflection of interfaces analytically, we introduce a piecewise linear system and we derive a ODE system, which is essentially 4-dimensional first order ODE, to descibe the dynamics of interfaces from the limiting problem by a formal expansion. By studying the ODEs, we make clear that very slowly travelling pulses has the nonannihilation property.
This section is essentially based on the results obtained in [11].

Section 4 : In §4.1, we consider the relation between stability of planar travelling pulse and velocity of travelling pulses for (1.1), (1.5). As a result, when very slowly travelling pulses exist, we show that planar travelling pulses are destabilized. In §4.2, we discuss the mechanism generating complex patterns. At first, we consider how expanding rings evolve when a travelling pulse has the nonannihilation property and planar instability. Form numerical computations, we find that the expanding rings break up into complex patterns, due to nonannihilation and planar instability of travelling pulses. As a result, we could expect that if very slowly travelling pulses exist, such complex patterns are generated by the nonannihilation property and planar instability. In order to confirm it, we again investigate the Gray-Scott model and obtain the same result as (1.1), (1.5). Therefore, we conclude that complex patterns are generated if very slowly travelling pulse solutions exist. In §4.3, we give a summary.

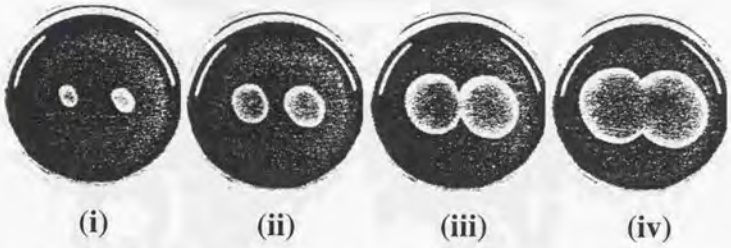

Figure 1.1: Annihilation of two expanding rings in the Belousov-Zhabotinsky reaction.

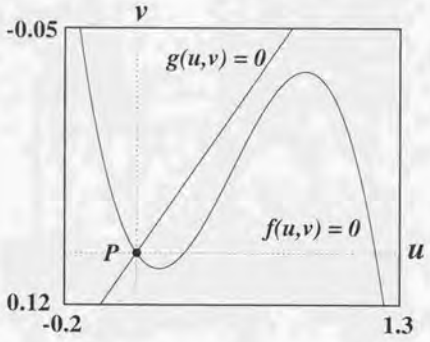

Figure 1.2: Nulclines of f and g with FitzHugh-Nagumo nonlinearities where $\gamma = 5.0, a = 0.2$.

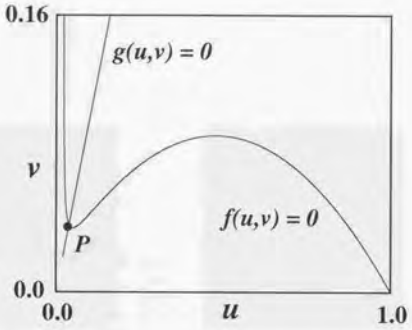

Figure 1.3: Nulclines of f and g with Oregonator nonlinearities where $\alpha = 3.0, q = 0.02$.

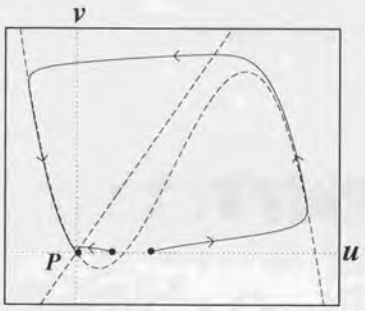

Figure 1.4: Trajectories of (1.1), (1.2) where $\gamma = 5.0, \varepsilon = 0.003, a = 0.2$.

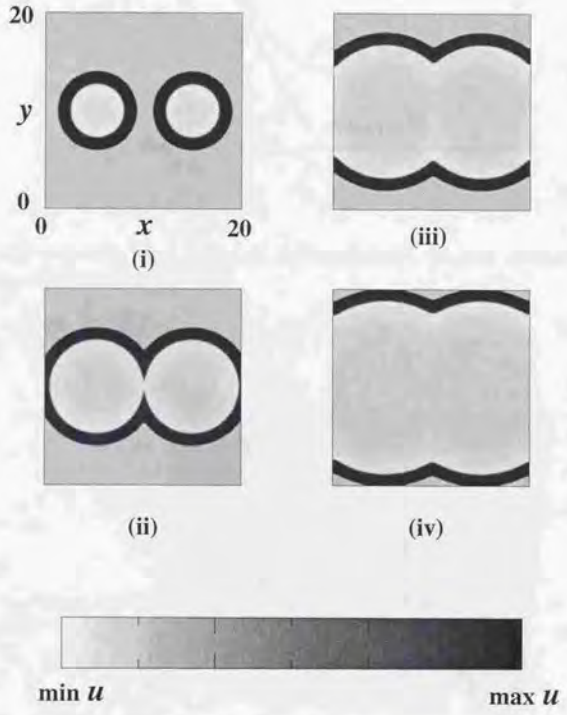

Figure 1.5: Annihilation of two ring patterns in a rectangle domain with zero flux boundary conditions. Spatio-temporal profile of u of (1.1), (1.2) where $\gamma = 5.0, \varepsilon = 0.00625, a = 0.25, d = 0.5$.

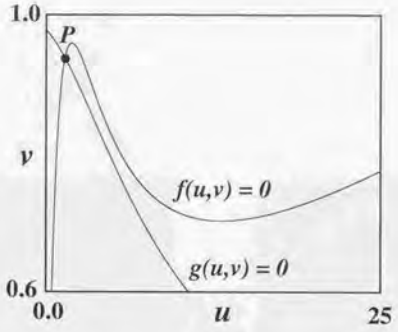

Figure 1.6: Nulclines of f and g of the exothermic reaction nonlinearities (1.5) where $a = 2.0, c = 5.0, h = 45.0, v_c = 1.0$

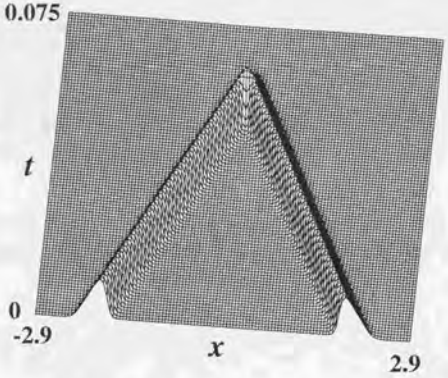

Figure 1.7: Annihilation of two travelling pulses of (1.1), (1.5) where $a = 2.0, c = 5.0, h = 45.0, v_c = 1.0, \varepsilon = 0.001, d = 0.5$.

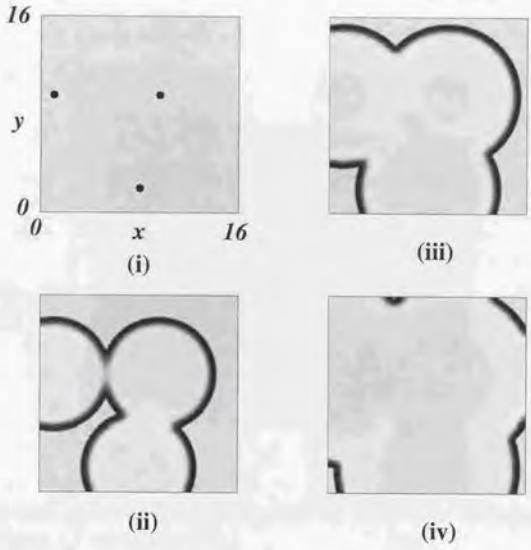

Figure 1.8: Annihilation of three expanding rings of (1.1), (1.5) in a rectangular domain with zero-flux boundary conditions where the parameters are the same as the ones in Figure 1.7.

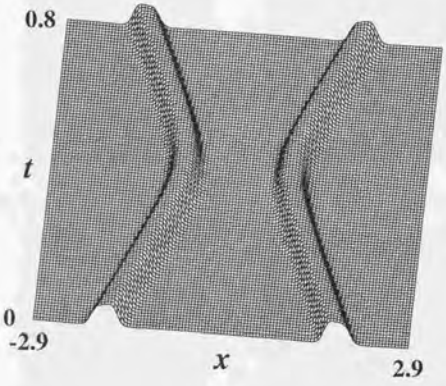

Figure 1.9: Reflection of two travelling pulses of (1.1), (1.5) where the parameters are same as the ones in Figure 1.7 except $d = 4.5$.

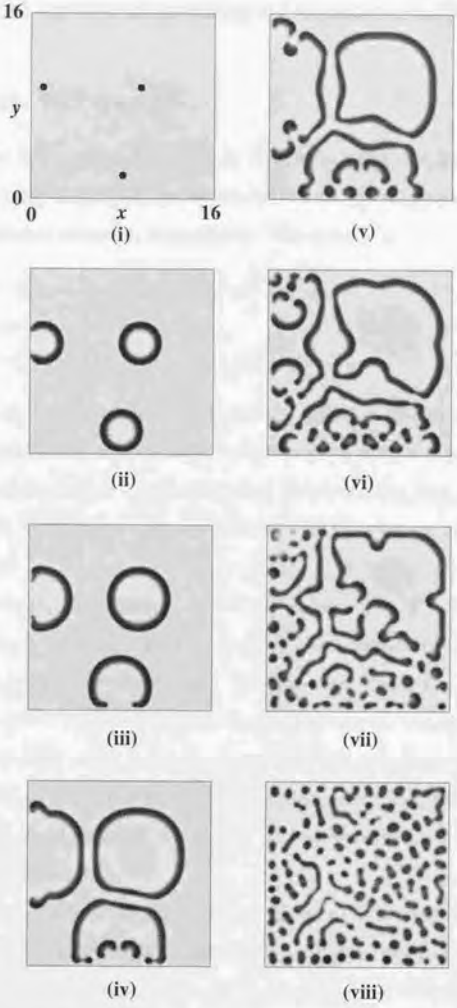

Figure 1.10: Breakdown of three ring patterns where the parameters are the same as the ones in Figure 1.9.

2 Numerical understanding of nonannihilation dynamics

2.1 Exothermic RD model

We propose here an RD system described in [12], which has the first order exothermic reaction. Let $u(t,x)$ and $v(t,x)$ be the dimensionless temperature and the dimensionless concentration of chemical reactant, respectively. The system is

$$(2.1)\qquad \begin{cases} \dfrac{\partial u}{\partial t} - \Delta u = \dfrac{1}{\varepsilon}(-au + k(u)v) \equiv \dfrac{1}{\varepsilon} f(u,v), \\ \dfrac{\partial v}{\partial t} - d\Delta v = (h(v_e - v) - k(u)v) \equiv g(u,v), \end{cases} \qquad t > 0, \quad x \in \boldsymbol{R}^n,$$

where d is the ratio of the heat conductivity and the diffusion rate of the reactant, ε is the time constant of two kinetics, a is the heat radiation rate, $k(u) = \exp(u/(1+u/c))$ is the reaction rate with some constant c, which is called the Arrhenius rate, h is the supply-rate of the reactant and v_e is the given concentration outside the system. All of the parameters are positive constants.

If c is small ($c < 4$), the function $v = F(u)$ obtained by $f(u,v) = 0$ is monotone increasing with u, if c is large ($c > 4$), it take cubic like nonlinearity (Figure 2.1). In this section, we fix c to satisfy the latter case. On the other hand, the function $v = G(u)$ obtained by $g(u,v) = 0$ is always monotone decreasing with u. For suitable values of a, h and v_e, curves of $v = F(u)$ and $v = G(u)$ are qualitatively classified into 4 cases. Figures 2.2a and 2.2b show that $v = F(u)$ and $v = G(u)$ have only one intersecting point, while Figures 2.2c and 2.2d do three ones. From now on, we restrict the nonlinearities f and g to satisfy the case of Figure 2.2a.

For computations in the following sections, we fix the parameters in (2.1) as $a = 2.0, h = 45.0, v_e = 1.0$ and $c = 5.0$ such that the nulclines of f and g are drawn in Fig.1.6 where there is uniquely one critical point, say $P = (u_p, v_p)$. We note that the solution $(u(t), v(t))$ of the diffusionless system to (2.1) possesses the property of excitability when ε is arbitrarily

fixed in the range of $\varepsilon = 0.0 \sim 0.002$, as in Figure 2.3. That is, our system satisfies (A-1) and (A-2).

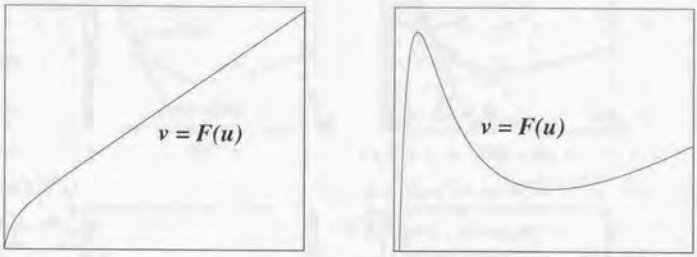

(a) (b)

Figure 2.1: Nulcline of f in (2.1): (a)$a = 2.0, c = 2.0$; (b)$a = 2.0, c = 5.0$.

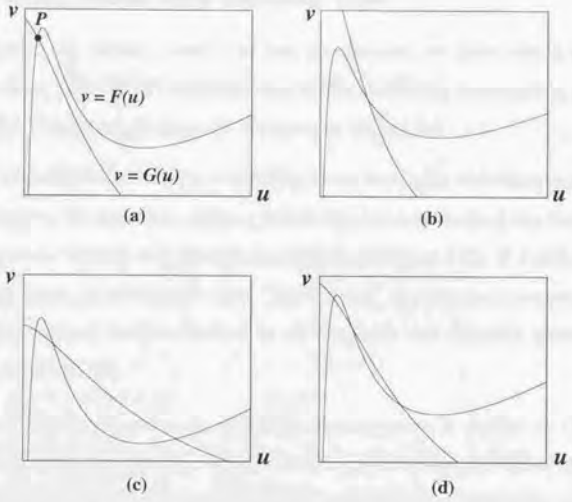

Figure 2.2: Nulclines of f and g in (2.1): (a) $a = 2.0, c = 5.0, h = 45.0, v_c = 1.0$; (b) $a = 1.5, c = 5.0, h = 20.0, v_c = 1.0$; (c) $a = 2.1, c = 5.0, h = 140.0, v_c = 1.0$; (d) $a = 2.0, c = 5.0, h = 65.0, v_c = 1.0$.

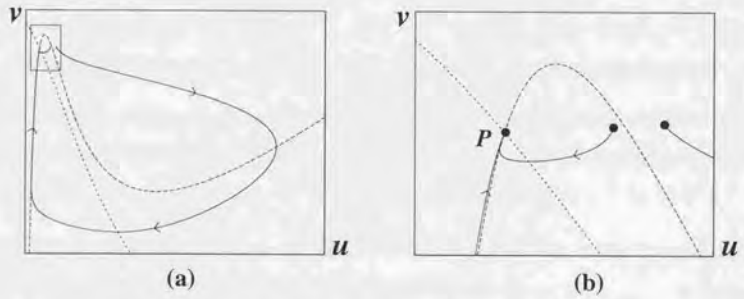

Figure 2.3: (a) Trajectories of (1.4), (1.5); (b) Detail of region near the critical point P where the parameters is the same as those in Figure 2.2a except $\varepsilon = 0.001$.

2.2 Travelling pulses and standing ones

In this subsection, by taking ε and d as free parameters, we draw the existence-regions of stable travelling pulse (STP) solutions and stable oscillating propagating pulse (SOPP) solutions of (2.1) in the (d, ε)-plane. It is shown in Figure 2.4.

(T-i) When ε is sufficiently small ($\varepsilon = 0.0003$), there is a stable travelling pulse for small d. If d increases, the travelling pulse is destabilized in a sense that the front propagates with constant velocity but the tail is oscillating (Figure 2.5). If d still increases, the travelling pulse is splitting so that "back firing" phenomenon occurs (Figure 2.6). Such phenomenon is also observed in an excitable and diffusive system with three critical points [1, 18].

(T-ii) When ε slightly increases ($\varepsilon = 0.001$), the situation is similar to (T-i) for small d. If d increases, the velocity of the travelling pulse becomes slower and it tends to a standing pulse. This indicates that the travelling pulse bifurcates super-critically from the standing one when d decreases.

(T-iii) When ε still slightly increases ($\varepsilon = 0.00125$), the situation is similar to (T-i) for small d. If d increases, there is an oscillating propagating pulse which is different from the one in (T-i) (Figure 2.7). If d still increases, there coexist an oscillating propagating pulse and a standing pulse. If d is large, there is a standing pulse only.

(T-iv) When ε slightly increases further ($\varepsilon = 0.0014$), the situation is similar to (T-i) for small d but if d increases, travelling pulses disappear. If d is large, there exist standing pulses only.

(T-v) When ε is not small, there are neither travelling pulses nor oscillating propagating ones for any d. There exist standing pulses for large d.

In order to understand why very slowly travelling pulses exist, we consider the cases of (T-ii) and (T-iii) more precisely. By numerically solving the 1-dimensional stationary problem

of (2.1), the global structure of standing pulse solutions can be drawn. When we fix $\varepsilon = 0.001$ (the case (T-ii))and take d as a free parameter, the structure of standing pulses is demonstrated in Figure 2.8, which it is stated as follows:

(S-i) There are two critical values $\underline{d}_c$, $\overline{d}_c$ such that there exist four standing pulses for $\underline{d}_c < d < \overline{d}_c$ (Figures 2.9a–2.9d).

(S-ii) There are two bifurcation points on the large branch where one is the translational bifurcation (TB) at $d = d_{TB}$ and the other is the oscillatory one (OB) at $d = d_{OB}$. The large solution is stable for $d_{TB} < d < \overline{d}_c$, while it is unstable for $\underline{d}_c < d < d_{TB}$ (see also Figure 2.8).

(S-iii) Other three branches are always unstable.

The existence region of large standing pulses in the (d, ε)-plane is demonstrated in Figure 2.10. One important remark is that TB and OB bifurcation curves intersect at one point in the (d, ε)-plane. Fix ε to be relatively small. When d decreases, TB occurs primarily and then OB dose secondary, and travelling pulses bifurcate super-critically from the standing one (Figure 2.11). This situation indicates two important facts: (i) There appear travelling pulses such that its velocity can be arbitrarily slow, as we want. If ε slightly increases, the locations of the TB and OB bifurcations is reverse. (ii) The existence of the intersecting point of the TB and OB bifurcation curves suggests the occurrence of secondary bifurcation by which stable oscillating propagating pulses appear, and there coexist stable oscillating propagating pulses and standing ones, as was stated in (T-iii). We should note that the TB and OB bifurcation curves never intersect for the FHN equations (1.1), (1.2).

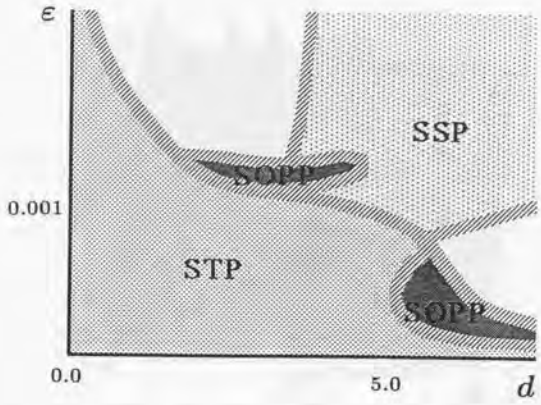

Figure 2.4: Existence region of stable travelling pulses(STP) and stable oscillating propagating pulses(SOPP) in the (ε, d)–plane.

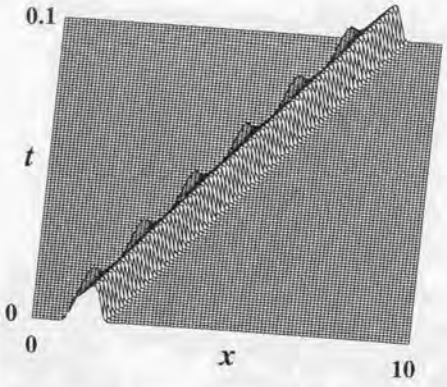

Figure 2.5: An oscillating propagating pulse where $\varepsilon = 0.0003, d = 9.5$.

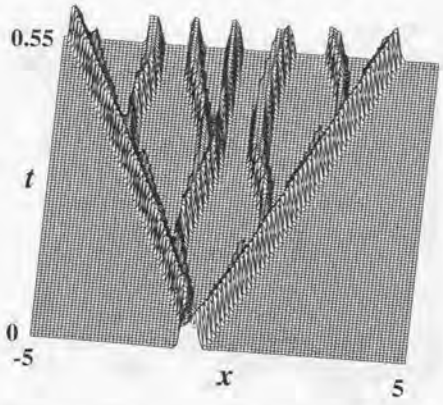

Figure 2.6: Back firing phenomenon where $\varepsilon = 0.0003, d = 13.0$.

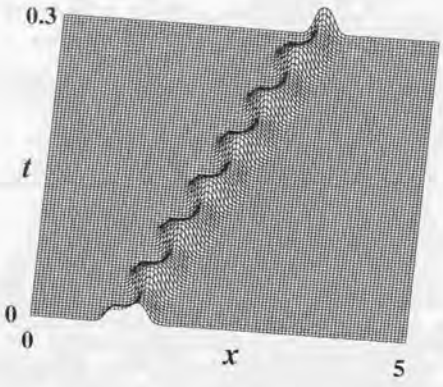

Figure 2.7: An oscillating propagating pulse where $\varepsilon = 0.0012, d = 3.5$.

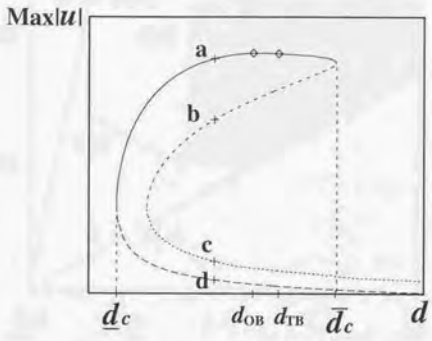

Figure 2.8: Global structure of standing pulses with the parameter d where $\varepsilon = 0.001$.

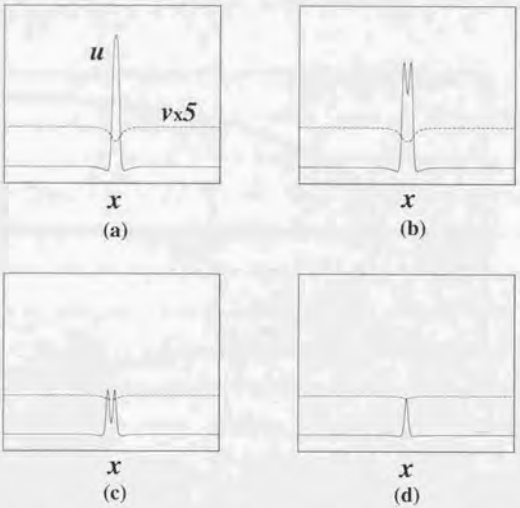

Figure 2.9: Spatial profiles of standing pulses where $\varepsilon = 0.001, d = 3.0$.

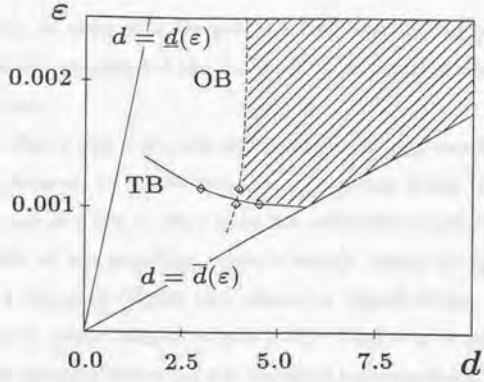

Figure 2.10: Existence region of standing pulses in the (ε, d)-plane where solid line is the curve of TB and dotted line is the curve of OB. Stable standing pulses are in the hatched region.

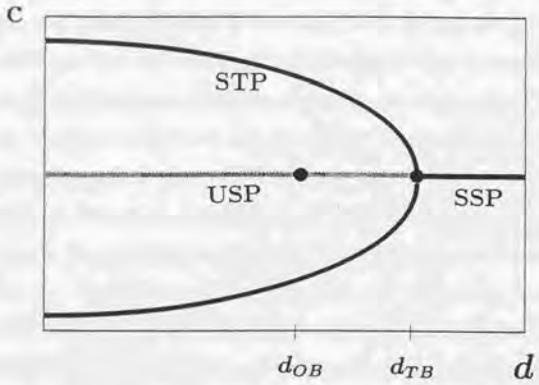

Figure 2.11: Bifurcation diagrams of travelling pulses with the parameter d:$\varepsilon = 0.001$, where the vertical axis indicates the velocity of the travelling pulse, SSP: stable standing pulse, USP: unstable standing pulse, STP: stable travelling pulse.

2.3 Nonannihilation dynamics of travelling pulses

In this subsection, we make clear the mechanism of nonannihilation property. As a first step, we consider the interaction of two travelling (or oscillating propagating) pulses which approach each other.

For the case when ε and d are both sufficiently small, two travelling pulses annihilate upon collision. However, we should note that annihilation occurs in two different types, depending on values of d and ε. Fix ε to be not sufficiently small. When d is sufficiently small, annihilation of two travelling pulses is exactly similar to the one arising in the FHN equations (1.1), (1.2) (Figure 1.7), when d is slightly larger, two pulses approach closely and fade out before collision (Figure 2.12). When d is increasing slightly further, such annihilation no longer occurs and two travelling pulses repel and move to the reversed direction (Figure 1.9). For the case when ε is slightly small and d is not so large, then there exists stable oscillating propagating pulses, which exhibit repulsion phenomenon (Figure 2.13).

The reason why nonannihilation of travelling pulses occurs has yet been unclear. One necessity condition is that the velocity of travelling pulses has to be slow. This is possible for the system (2.1), because the bifurcation from the standing pulse to the travelling one is super-critical. We thus can choose ε and d such that the velocity is arbitrarily slow. When two slowly travelling pulses approach closely, the concentration of the reactant between two pulses becomes lower than ones in the back part of the pulses so that they repel each other and move to the opposite direction, recovering their shapes(Figure 2.14). We should note here that for the FHN equations (1.1),(1.2), the bifurcation is always sub-critical, even if the translational bifurcation primarily occurs [9]. Therefore, the existence of slowly travelling pulses can not be expected and the resulting two travelling pulses annihilate, as is observed in the BZ reactions and in the FHN equations.

Thus, we can expect that it is essential for the occurrence of nonannihilation of travelling pulses that the velocity is very slow. In order to confirm it, we consider the following more

general 2-component system of (2.1):

$$
\begin{cases}
\dfrac{\partial u}{\partial t} - \Delta u = \dfrac{1}{\varepsilon}(-au + p(u)v) \equiv \dfrac{1}{\varepsilon} f(u,v), \\
\dfrac{\partial v}{\partial t} - d\Delta v = h(v_c - v) - p(u)v \equiv g(u,v),
\end{cases}
\qquad t > 0, \quad \boldsymbol{R}^n, \tag{2.2}
$$

where a, h, and v_c are positive constants. Take $p(u) = u^m$ (m is positive integer). If $m = 1$, (2.2) never takes excitability, while if $m \geq 2$, it takes mono-stable excitability for suitable a, h and v_c, though $f(u,v) = 0$ dose not exhibit cubic nonlinearity. In fact when $p(u) = u^2$, for which (2.2) is known as the Gray-Scott model, it is shown in Figure 2.15. It is confirmed that there is the TB bifurcation curves so that travelling pulses bifurcate super-critically from the standing ones when d is suitably fixed and ε decreases (Figure 2.16). This is qualitatively similar to the one in Figure 2.10. Moreover, nonannihilation of slowly travelling pulses are also shown in Figure 2.17. This phenomena are also observed in (2.2) with $p(u) = \exp(u)$.

As travelling pulses, which exist for suitably large d, bifurcate primarily and super-critically from standing ones, we can expect that this travelling pulses have lateral inhibition property. Now, we explain lateral inhibition for (2.1) as follows: if the diffusion of v is larger than that of u then v, as it gets "consumed" in the reaction region, diffuses in the consumption region. Therefore, before u expands laterally, the value of v around the reacting region becomes small. Thus, the expansion of u is inhibited in the sense that the velocity of expansion becomes very small. This property is called *lateral inhibition*.

By the above discussion, we arrived at the following:

(C-1) If very slowly travelling pulses with lateral inhibition exist for any 2-component system, they repel each other.

Through this paper, we shall assume that very slowly travelling pulse is under lateral inhibition unless otherwise stated.

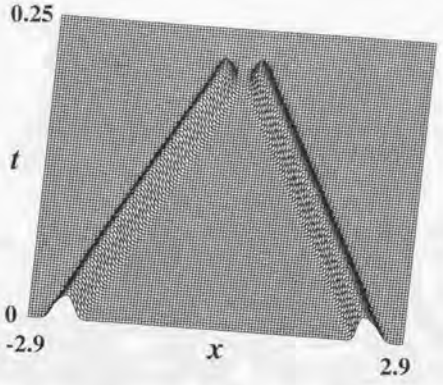

Figure 2.12: Extinction before collision where $\varepsilon = 0.001, d = 3.1$.

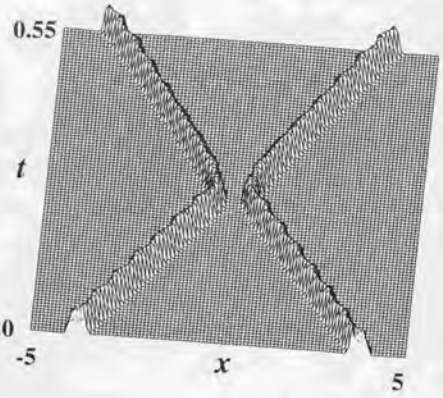

Figure 2.13: Reflection of two oscillating propagating pulses of (2.1) where $\varepsilon = 0.0006, d = 7.0$.

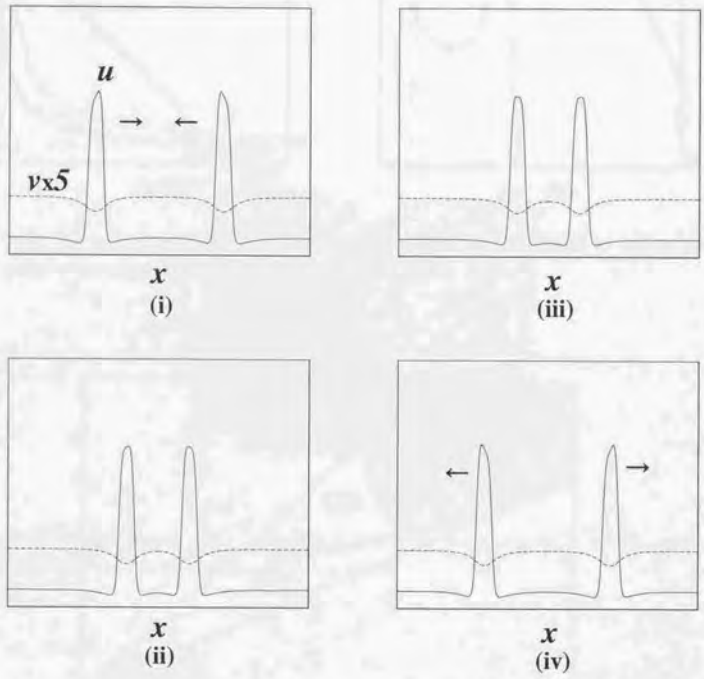

Figure 2.14: Non-annihilation process of two travelling pulses where $\varepsilon = 0.001, d = 4.5$.

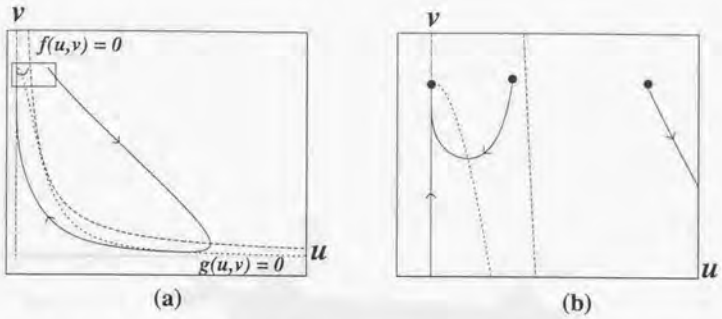

Figure 2.15: (a) Trajectories of the Gray-Scott model (2.2); (b) Detail of region near the critical point where $a = 0.07, h = 0.018, v_c = 1.0, \varepsilon = 0.8$.

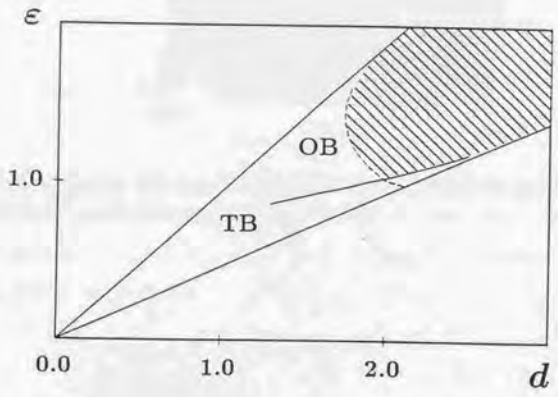

Figure 2.16: Existence region of standing pulse in the (d, ε)-plane where the sold line is the curve of TB and the dotted line is the curve of OB. Stable standing pulses are in the hatched region.

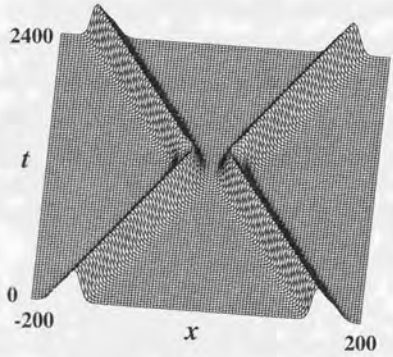

Figure 2.17: Reflection of two travelling pulses of (2.2) where the parameters are the same as the ones in Figure 2.14 except $\varepsilon = 1.0, d = 3.5$.

3 Analytical understanding of nonannihilation dynamics

3.1 A bistable RD system

The aim of this section is to show analytically that (C-1) holds. If ε is sufficiently small in system (2.1), the velocity of travelling pulses are so fast as shown in Figure 3.1 that two travelling pulses annihilate (Figure 3.2). For this situation, we do not have any analytical tools to solve the system (2.1) yet. Thus, we give up treating system (2.1). So we found a bistable RD system as one having slowly travelling pulse under the situation that ε is sufficiently small. Thus, by using a singular perturbation method, we can define the positions of travelling pulse as the two interfaces, which we call front and back. Accordingly, we can consider the problem of the reflection for the interfaces. Therefore, we discuss the repulsive phenomenon about the following 1-dimensional bistable FHN system [19]:

$$\begin{cases} \varepsilon\tau\dfrac{\partial u}{\partial t} = \varepsilon^2\dfrac{\partial^2 u}{\partial x^2} + f(u) - v, \\ \dfrac{\partial v}{\partial t} = d\dfrac{\partial^2 v}{\partial x^2} + u - \gamma v \end{cases} \qquad t > 0, \quad x \in \boldsymbol{R}, \tag{3.1}$$

with $f(u) = u(1-u)(u-a)$, where ε, τ, d, a and γ are positive constants, ε is sufficiently small and $0 < a < 1/2$. We assume that the curves $f(u) - v = 0$ and $u - \gamma v = 0$ have three intersection points, say P, Q and R, as in Figure 3.3 where P and R are the stable constant equilibrium solutions of (3.1), while Q is the unstable one. We impose the boundary conditions to (3.1) as

$$(u, v)(t, \pm\infty) = P. \tag{3.2}$$

Let $\gamma = \gamma_*$ be given such that the curves $f(u) - v = 0$ and $u - \gamma_* v = 0$ take odd symmetry with respect to the point Q in the (u, v)-plane. We assume that γ is chosen to be near but less than γ_* such that the curves $f(u) - v = 0$ and $u - \gamma v = 0$ take nearly odd symmetry with respect to Q. Under this situation, it was shown that (3.1),(3.2) has travelling pulse

solutions for suitably small τ [6]. The feature of these solutions is that there are one front and one back layers in u and the distance between them is rather long, as in Figure 3.4. We consider the interaction of these two travelling pulses which are symmetric with $x = 0$. When τ is very small, the travelling pulses annihilate on collision (Figure 3.5). If τ increases, the velocity becomes slower and two pulses fade out before collision (Figure 3.6) and if τ still increases slightly, they repel each other in such a way that two travelling front layers repel each other twice, while the back layers do once (Figure 3.7). The repulsive process is different from the one in the exothermic RD system (2.1), as was shown in Figure 1.9. Nevertheless, it is thus numerically confirmed that very slowly travelling pulse solutions of (3.1),(3.2) possess nonannihilation property when ε is sufficiently small.

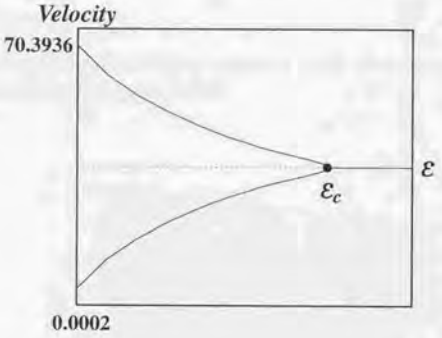

Figure 3.1: Relation between the velocity c of travelling pulses of (2.1) and the parameter ε where the parameters is the same as those in Figure 1.9 and $\varepsilon_c = 0.001027$.

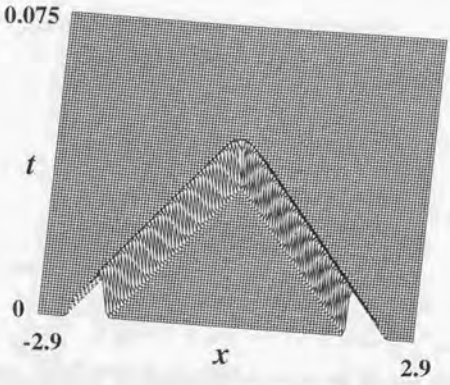

Figure 3.2: Annihilation of two travelling pulses of (2.1) where the parameters are the same as those in Figure 1.9 except $\varepsilon = 0.0003$.

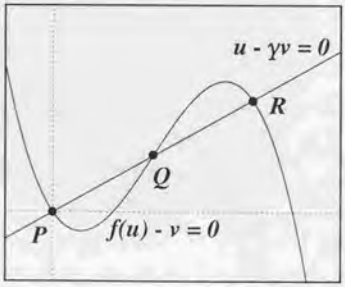

Figure 3.3: Nulclines of f and g with FitzHugh-Nagumo nonlinearities where $a = 0.25, \gamma = 10.2857$.

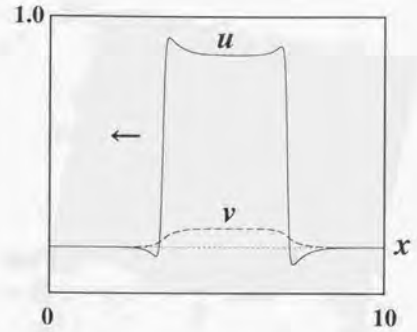

Figure 3.4: A travelling pulse of (3.1) where d = 1.0, $a = 0.25, \gamma = 10.2857, \tau = 0.046, \varepsilon = 0.025$.

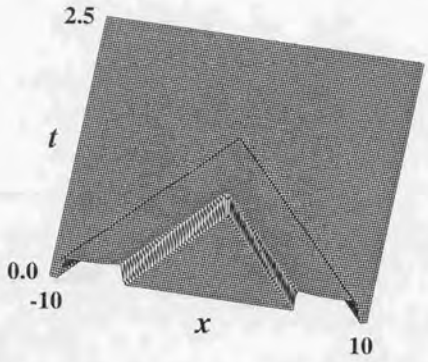

Figure 3.5: Annihilation of two travelling pulses of (3.1) where the parameters are the same as those in Figure 3.4 except $\tau = 0.035$.

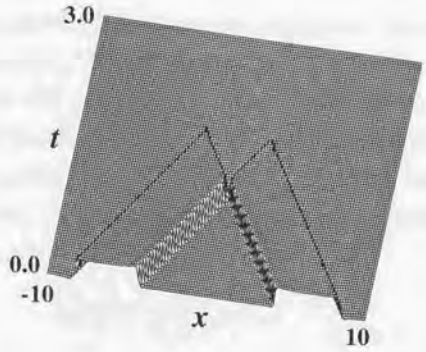

Figure 3.6: Annihilation of two travelling pulses of (3.1) where the parameters are the same as those in Figure 3.4 except $\tau = 0.04311$.

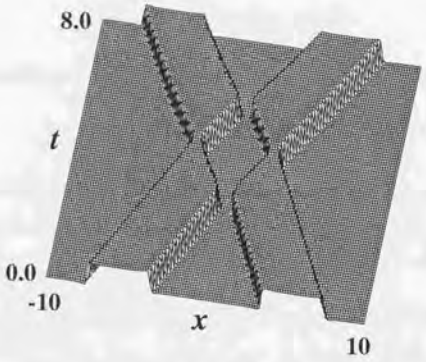

Figure 3.7: Repulsion of two travelling pulses of (3.1) where the parameters are the same as those in Figure 3.4 except $\tau = 0.048$.

3.2 Limiting system (3.1),(3.2) as $\varepsilon \downarrow 0$

In order to define the position of travelling pulses in (3.1) with (3.2), we derive the limiting system as $\varepsilon \downarrow 0$ from (3.1). Taking the limit as $\varepsilon \downarrow 0$, we consider the dynamics of one pulse-like solution with one front and one back layers moving to the left direction, of the 1-dimensional bistable FHN system (3.1), (3.2) in $\boldsymbol{R}$ (Figure 3.8). Let $\eta_F(t)$ and $\eta_B(t)$ $(0 < \eta_F(t) < \eta_B(t))$ be the interfaces corresponding the front and back layers of the solution (Figure 3.9). By using singular perturbation methods ([14], for instance), the equations for $\eta_F(t), \eta_B(t)$ and $v(t,x)$ are given by

$$\tau \dot{\eta_F}(t) = -\lambda(v(t, \eta_F(t))), \quad t > 0, \tag{3.3}$$

$$\tau \dot{\eta_B}(t) = \lambda(v(t, \eta_B(t))), \quad t > 0, \tag{3.4}$$

where dot means the first derivative with respect to time t. Here $\lambda(\xi)$ is the velocity of a travelling front solution $u(z)$ $(z = x - \lambda t)$ of

$$u_t = u_{xx} + f(u) - \xi, \quad z \in \boldsymbol{R} \tag{3.5}$$

with the boundary conditions

$$\lim_{x \to \pm\infty} u(t,x) = h_{\mp}(\xi), \tag{3.6}$$

where ξ is suitably fixed such that $f(u) - \xi = 0$ has three zeros $u = h_{\pm}(\xi)$ and $h_0(\xi)$, as in Figure 3.10. $\lambda(\xi)$ has the explicit expression $\lambda(\xi) = (h_+(\xi) + h_-(\xi) - 2h_0(\xi))/\sqrt{2}$. From (3.1), the equation for $v(t,x)$ is given by

$$\frac{\partial v}{\partial t} = d\frac{\partial^2 v}{\partial x^2} + \begin{cases} h_-(v) - \gamma v, & t > 0, \quad x \in \boldsymbol{R} \setminus (\eta_F(t), \eta_B(t)), \\ h_+(v) - \gamma v, & t > 0, \quad x \in (\eta_F(t), \eta_B(t)) \end{cases} \tag{3.7}$$

with

$$v(t,\cdot) \in C^1(\boldsymbol{R}), \quad t > 0 \tag{3.8}$$

and

$$\lim_{|x|\to\infty} v(t,x) = 0, \quad t > 0. \tag{3.9}$$

The derivation of (3.3)-(3.9) is stated in Appendix A.

For a special solution of (3.3)-(3.9), there are travelling pulse solutions $v(t,x) = V(z)$ $(z = x - ct)$ with constant velocity c, coupled with the interfaces $\eta_F(t) = z_F = x_F - ct$ and $\eta_B(t) = z_B = x_B - ct$ (Figure 3.11). The problem for $(V(z), c)$ resulting from (3.3)-(3.9) is

$$-\tau c = -\lambda(V(z_F)) = \lambda(V(z_B)), \tag{3.10}$$

$$-cV_z = dV_{zz} + \begin{cases} h_-(V) - \gamma V, & z \in \boldsymbol{R} \setminus (z_F, z_B), \\ h_+(V) - \gamma V, & z \in (z_F, z_B), \end{cases} \tag{3.11}$$

$$V \in C^1(\boldsymbol{R}), \tag{3.12}$$

and

$$\lim_{|z|\to\infty} V(z) = 0. \tag{3.13}$$

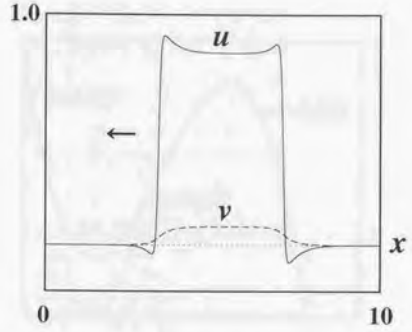

Figure 3.8: A travelling pulse of (3.1) where the parameters are the same as those in Figure 3.4 except $\tau = 0.04455$

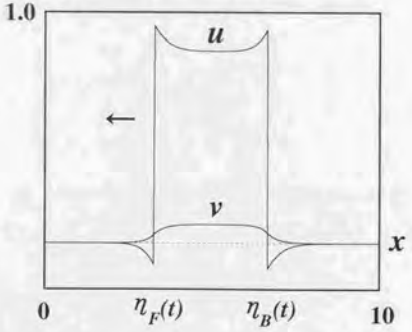

Figure 3.9: A travelling pulse of (3.1) for $\varepsilon \downarrow 0$ where the parameters are the same as those in Figure 3.8.

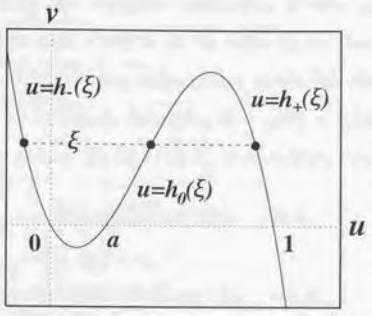

Figure 3.10: Graph of the equation $f(u)-v=0$, where $u=h_-(v), u=h_+(v)$ and $u=h_0(v)$ denote three branches of $f(u)-v=0$.

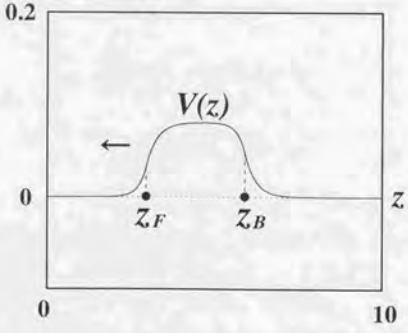

Figure 3.11: A travelling pulse solution $V(z)$ of (3.10)-(3.13) where $d=1.0, a=0.25, \gamma=10.28571, \tau=0.044$.

3.3 Pulse-interaction in the limiting system

In this subsection, we study the repulsive interaction of two travelling pulses of (3.10)-(3.13) which are symmetric with $x = 0$ in $\boldsymbol{R}$. In order to do this, we assume that there is the reflecting wall at $x = 0$ so that one pulse moves to the left direction in $\boldsymbol{R}_+ = (0, +\infty)$. Let $x = \eta_1(t), x = \eta_2(t)$ be interfaces satisfying $0 < \eta_2(t) < \eta_1(t) < +\infty$, where $2\eta_2(t)$ is the distance between two pulses. By (3.3)-(3.9), the problem can be stated as follows:

$$\tau\dot{\eta}_1 = \lambda(v(t, \eta_1(t))), \quad t > 0, \tag{3.14}$$

$$\tau\dot{\eta}_2 = -\lambda(v(t, \eta_2(t))), \quad t > 0, \tag{3.15}$$

$$\frac{\partial v}{\partial t} = d\frac{\partial^2 v}{\partial x^2} + \begin{cases} h_-(v) - \gamma v, & t > 0, x \in \boldsymbol{R}_+ \setminus (\eta_2(t), \eta_1(t)), \\ h_+(v) - \gamma v, & t > 0, x \in (\eta_2(t), \eta_1(t)), \end{cases} \tag{3.16}$$

$$v(t, \cdot) \in C^1(\boldsymbol{R}_+) \tag{3.17}$$

with the boundary and initial conditions

$$\frac{\partial v}{\partial x} = 0, \quad t > 0, x = 0, \tag{3.18}$$

$$\lim_{x \to +\infty} v = 0, \quad t > 0, \tag{3.19}$$

and

$$\begin{array}{rcl} \eta_1(0) & = & \eta_{10}, \\ \eta_2(0) & = & \eta_{20}, \\ v(0, x) & = & v_0(x), \quad x \in \boldsymbol{R}_+, \end{array} \tag{3.20}$$

where $v_0(x)$, η_{10} and η_{20} are approximately chosen as the travelling pulse solution $V(x)$ with velocity $-c(\tau)$ and the interfaces x_B and x_F of (3.10)-(3.13), by taking x_B and x_F very large. This indicates that the solution $(v(t, x), \eta_1(t), \eta_2(t))$ initially takes a travelling pulse with velocity $-c(\tau)$.

The convergence of solutions of the RD system (3.1) to the ones of (3.14)-(3.20) as $\varepsilon \downarrow 0$ is discussed in [23]. Also the existence and uniqueness of solutions to (3.14)-(3.20) are proved in [5]. Our problem can be stated as follows: do the interfaces $\eta_i(t)$ $(i = 1, 2)$ of (3.14)-(3.20) exhibit repulsive processes when τ is taken such that $c(\tau)$ is very small? In order to confirm it, we numerically solve the limiting problem (3.14)-(3.20) for different values of τ. Figures 3.12 and 3.13 show the annihilation of two travelling interfaces after and before collision, respectively. On the other hand, when the velocity $c(\tau)$ is very slow, Figure 3.14 demonstrates the repulsion of travelling pulses. One thus finds that the pulse-pulse interactions in the limiting problem (3.14)-(3.20) are qualitatively similar to the ones in the bistable FHN system (3.1),(3.2) with sufficiently small $\varepsilon > 0$, as was shown in Figures 3.5-3.7.

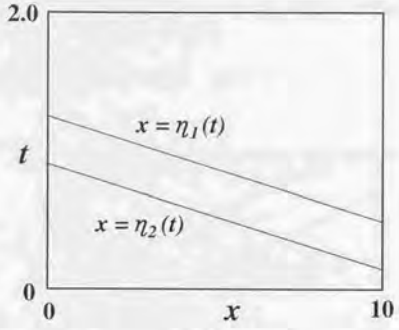

Figure 3.12: Annihilation of travelling pulses of (3.14)-(3.20) where $d = 1.0, a = 0.25, \gamma = 10.28571, \tau = 0.034$.

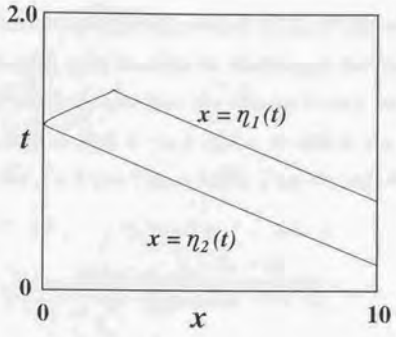

Figure 3.13: Annihilation of travelling pulses of (3.14)-(3.20) where the parameters are the same as those in Figure 3.12 except $\tau = 0.0375$.

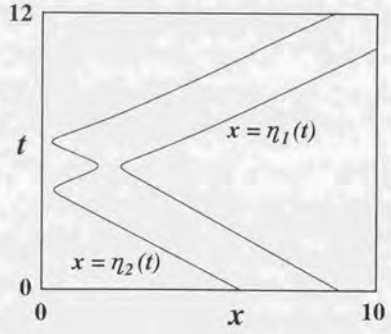

Figure 3.14: Repulsion of travelling pulses of (3.14)-(3.20) where the parameters are the same as those in Figure 3.12 except $\tau = 0.044$.

3.4 Equations of interface-interface interaction

In this subsection, we reduce the limiting problem (3.14)-(3.20) to a system of ODEs for the interfaces $\eta_1(t)$ and $\eta_2(t)$ only, in order to understand the mechanism how repulsive interaction of travelling pulses occurs when the velocity is very slow.

We specify $f(u)$ in (3.1) as $f(u) = -u + H(u-a)$ with $0 < a < 1/2$ where $H(s) = 1$ for $s > 0$ and $H(s) = 0$ for $s < 0$ (see Figure 3.15). Then the velocity $\lambda(\xi)$ of (3.5) is given by

$$\lambda(\xi) = \frac{1-2a-2\xi}{\sqrt{(a+\xi)(1-a-\xi)}} \tag{3.21}$$

[19] or equivalently

$$\frac{\lambda(\xi)}{\sqrt{\lambda^2(\xi)+4}} = 1-2a-2\xi. \tag{3.22}$$

We first obtain travelling pulse solutions $(V(z), c)$ with $z = x - ct$. The resulting problem (3.10)-(3.13) is

$$\frac{\tau c}{\sqrt{(\tau c)^2+4}} = 1-2a-2V(z_F), \tag{3.23}$$

$$\frac{\tau c}{\sqrt{(\tau c)^2+4}} = -1+2a+2V(z_B) \tag{3.24}$$

and with $\beta = 1+\gamma$,

$$-cV_z = dV_{zz} + \begin{cases} -\beta V, & x \in \boldsymbol{R} \setminus (z_F, z_B), \\ -\beta V + 1, & x \in (z_F, z_B), \end{cases} \tag{3.25}$$

$$V \in C^1(\boldsymbol{R}), \tag{3.26}$$

and

$$\lim_{|z|\to\infty} V(z) = 0. \tag{3.27}$$

Solving (3.25)-(3.27) to obtain the unknown V for fixed c and $z_B - z_F = s$, and substituting it into (3.23),(3.24), we have the following equations for c and s:

$$\frac{\tau c}{\sqrt{(\tau c)^2+4}} = 1 - 2a - \frac{\phi_-}{\beta\phi}\left(1 - \exp(-\frac{\phi_+}{2d}s)\right), \tag{3.28}$$

$$\frac{\tau c}{\sqrt{(\tau c)^2+4}} = -1 + 2a + \frac{\phi_+}{\beta\phi}\left(1 - \exp(-\frac{\phi_-}{2d}s)\right), \tag{3.29}$$

where $\phi(c) = \sqrt{c^2+4d\beta}$ and $\phi_\pm(c) = \phi(c) \pm c$. It is convenient to rewrite (3.28),(3.29) as

$$F(c,s) = \frac{\phi_-}{2\beta\phi}\exp(-\frac{\phi_+}{2d}s) + \frac{\phi_+}{2\beta\phi}\exp(-\frac{\phi_-}{2d}s) - 2a - \frac{1}{\beta} + 1 = 0, \tag{3.30}$$

$$G(c,s;\tau) = \frac{\tau c}{\sqrt{(\tau c)^2+4}} - \frac{c}{\beta\phi} - \frac{\phi_-}{2\beta\phi}\exp(-\frac{\phi_+}{2d}s) + \frac{\phi_+}{2\beta\phi}\exp(-\frac{\phi_-}{2d}s) = 0. \tag{3.31}$$

When $2a + 1/\beta - 1 = 0$ (or $\gamma = \gamma_* = 2a/(1-2a)$), we note that $f(u) - v = 0$ and $u - \gamma_* v = 0$ take odd symmetry. When $2a + 1/\beta - 1 \le 0$ (or $\gamma \ge \gamma_*$), $F(c,s) > 0$ holds so that (3.30), (3.31) have no solution for any c and s. We therefore assume $2a + 1/\beta - 1 > 0$ (or $0 < \gamma < \gamma_*$). It is obvious that $(c,s) = (0,s_0)$ with $s_0 = -\sqrt{d/\beta}\log(2a\beta + 1 - \beta)$ is a solution of (3.30),(3.31) for any $\tau > 0$. This means that there is a standing pulse for any $\tau > 0$. To obtain travelling pulse solutions of (3.30), (3.31), we have to rely on numerical computation. By taking τ as a free parameter and keeping $a, \gamma(<\gamma_*)$ and d to be suitably fixed, we find that there is the critical value τ_{cT} such that travelling pulses exist for $\tau < \tau_{cT}$, which are bifurcated from the standing one at $\tau = \tau_{cT}$ (Figure 3.16). The relation between τ and the width s are also shown in Figure 3.17.

If τ is chosen to be near τ_{cT}, the velocity c is very small so that its explicit form can be shown. Using $F(0,s_0) = 0$ and $\dfrac{\partial F}{\partial s}(0,s_0) \neq 0$, the implicit function theorem says that $F(c,s) = 0$ has a solution $s = h(c)$ in a neighborhood of $c = 0$ satisfying $s_0 = h(0)$. We note that $s = h(c)$ is expanded in terms of c up to $O(c^2)$

$$s = h(c) = s_0 + s_1 c^2, \tag{3.32}$$

where

$$s_1 = \frac{1}{16}\left(\frac{s_0}{d\beta} + \frac{s_0^2}{d\sqrt{d\beta}}\right).$$

Substituting (3.32) into $G(c, s; \tau) = 0$ and expanding it with respect to small c, we obtain the following relation up to $O(c^3)$:

$$\frac{c}{2}(\tau - \tau_*) + gc^3 = 0, \tag{3.33}$$

where

$$\tau_* = \frac{1}{\beta\sqrt{d\beta}}\left(1 - \left(1 + s_0\sqrt{\beta/d}\right)\exp(-s_0\sqrt{\beta/d})\right) > 0, \tag{3.34}$$

which is near τ_{cT} and

$$g(\tau) = \frac{1}{16}\Big[\frac{1}{d\beta^2\sqrt{d\beta}} + \left(\frac{s_0^3}{3d^3\beta} - \frac{s_0}{d^2\beta^3} - \frac{1}{d\beta^2\sqrt{d\beta}} - \frac{8s_0s_1}{d\sqrt{d\beta}}\right)\exp(-\sqrt{\beta/d}s_0) - \tau^3\Big]. \tag{3.35}$$

When γ is near γ_* and τ is also near τ_*, one finds $g(\tau) > 0$. Therefore the velocity c is expressed as $c = \pm\sqrt{(\tau_* - \tau)/2g(\tau)}$ for small c.

The spectral analysis [6] shows that when τ decreases, the standing pulse solution of (3.3)-(3.9) is destabilized primarily through Hopf bifurcation at $\tau = \tau_{cO}$ and then secondly through translational one at $\tau = \tau_{cT}$ $(\tau_{cT} < \tau_{cO})$. This implies that travelling pulse solutions are unstable when τ is near τ_{cT}, though they exist for $\tau < \tau_{cT}$. However, we should remark that there is the critical value τ_{cOT} $(\tau_{cOT} < \tau_{cT})$ so that the unstable travelling pulse solution recovers its stability for $\tau < \tau_{cOT}$ (Figure 3.18) [7]. It is also noted that if γ is less than but near γ_* (i.e. the kinetics $f(u) - v = 0$ and $u - \gamma v = 0$ take nearly odd symmetry), three critical values τ_{cOT}, τ_{cT} and τ_{cO} are very close with each other (if they are completely odd symmetric, $\tau_{cOT} = \tau_{cT} = \tau_{cO}$ hold). We thus find that there exist very slowly travelling pulse solutions which are stable, if γ is near γ_* and τ is also near τ_{cOT}.

We now study the repulsive interaction of two very slowly travelling pulse solutions obtained above. Consider the situation where these two travelling pulses are symmetric

with respect to $x = 0$ in $\boldsymbol{R}$. The problem resulting from (3.14)-(3.20) with (3.21) is written as

$$\frac{\tau\dot{\eta}_1(t)}{\sqrt{(\tau\dot{\eta}_1(t))^2+4}} = 1 - 2a - 2v(t,\eta_1(t)), \quad t > 0, \tag{3.36}$$

$$\frac{\tau\dot{\eta}_2(t)}{\sqrt{(\tau\dot{\eta}_2(t))^2+4}} = -1 + 2a + 2v(t,\eta_2(t)), \quad t > 0, \tag{3.37}$$

$$\frac{\partial v}{\partial t} = d\frac{\partial^2 v}{\partial x^2} + \begin{cases} -\beta v, & x \in \boldsymbol{R}_+ \setminus (\eta_2(t), \eta_1(t)), \\ -\beta v + 1, & x \in (\eta_2(t), \eta_1(t))), \end{cases} \tag{3.38}$$

$$v(t,\cdot) \in C^1(\boldsymbol{R}_+), \tag{3.39}$$

$$\frac{\partial v}{\partial x} = 0, \quad x = 0, \quad t > 0, \tag{3.40}$$

$$\lim_{x\to\infty} v = 0, \quad t > 0, \tag{3.41}$$

$$\begin{aligned} &\eta_1(0) = \eta_{10}, \\ &\eta_2(0) = \eta_{20} \quad (< \eta_{10}), \\ &v(0,x) = v_0(x), \quad x \in \boldsymbol{R}_+. \end{aligned} \tag{3.42}$$

By using the advantage of piecewise-linear nonlinearity of (3.23), $v(t,\eta_i(t))$ $(i = 1,2)$ can be determined by solving (3.38) for given $\eta_i(t)$ $(i = 1,2)$. We thus formally obtain the closed system for $\eta_1(t)$ and $\eta_2(t)$, which is described by integral equations with respect to time as well as space. Its treatment is therefore generally difficult. In order to avoid this difficulty, we employ the following approximation:

$$\eta_i(s) = \eta_i(t) + (s-t)\dot{\eta}_i(t) + \frac{(s-t)^2}{2}\ddot{\eta}_i(t) + \cdots, \tag{3.43}$$

which is valid for sufficiently weak variation of η_i $(i = 1,2)$. The validity of (3.43) is stated in Appendix C. After straightforward calculation, we obtain the following 4-dimensional ODEs for $\eta_1(t)$ and $\eta_2(t)$ from (3.36)-(3.42) up to $O(\ddot{\eta}_i)$ $(i = 1,2)$:

$$m(\eta_1,\dot{\eta}_1)\ddot{\eta}_1 - n_1(\eta_1,\eta_2,\dot{\eta}_2)\ddot{\eta}_2 = 1 - 2a - v_1(\eta_1,\eta_2,\dot{\eta}_1,\dot{\eta}_2) - \frac{\tau\dot{\eta}_1}{\sqrt{(\tau\dot{\eta}_1)^2+4}}, \quad t > 0, \tag{3.44}$$

(3.45) $m(\eta_2,\dot\eta_2)\ddot\eta_2 - n_2(\eta_1,\eta_2,\dot\eta_1)\ddot\eta_1 = -1+2a+v_2(\eta_1,\eta_2,\dot\eta_1,\dot\eta_1) - \dfrac{\tau\dot\eta_2}{\sqrt{(\tau\dot\eta_2)^2+4}},\quad t>0,$

where for $\phi_i = \phi(\dot\eta_i) = \sqrt{\dot\eta_i{}^2 + 4d\beta}$ and $\phi_{i\pm} = \phi(\dot\eta_i) \pm \dot\eta_i$ $(i=1,2)$,

$$
\begin{aligned}
m(\eta_i,\dot\eta_i) &= \frac{12d^2}{\phi_i^5}\left(1+\exp(-2\eta_i\frac{\phi_{i-}}{2d})\right)\\
&\quad + \left(\frac{4\eta_i^2}{\phi_i^3}+\frac{12d\eta_i}{\phi_i^4}\right)\exp(-2\eta_i\frac{\phi_{i-}}{2d}) \quad (i=1,2),
\end{aligned}
\tag{3.46}
$$

$$
\begin{aligned}
n_1(\eta_1,\eta_2,\dot\eta_2) &= \left(\frac{(\eta_1-\eta_2)^2}{\phi_2^3}+\frac{6d(\eta_1-\eta_2)}{\phi_2^4}+\frac{12d^2}{\phi_2^5}\right)\exp(-(\eta_1-\eta_2)\frac{\phi_{2+}}{2d})\\
&\quad + \left(\frac{(\eta_1+\eta_2)^2}{\phi_2^3}+\frac{6d(\eta_1+\eta_2)}{\phi_2^4}+\frac{12d^2}{\phi_2^5}\right)\exp(-(\eta_1+\eta_2)\frac{\phi_{2-}}{2d}),
\end{aligned}
\tag{3.47}
$$

$$
\begin{aligned}
n_2(\eta_1,\eta_2,\dot\eta_1) &= \left(\frac{(\eta_1-\eta_2)^2}{\phi_1^3}+\frac{6d(\eta_1-\eta_2)}{\phi_1^4}+\frac{12d^2}{\phi_1^5}\right)\exp(-(\eta_1-\eta_2)\frac{\phi_{1-}}{2d})\\
&\quad + \left(\frac{(\eta_1+\eta_2)^2}{\phi_1^3}+\frac{6d(\eta_1+\eta_2)}{\phi_1^4}+\frac{12d^2}{\phi_1^5}\right)\exp(-(\eta_1+\eta_2)\frac{\phi_{1-}}{2d}),
\end{aligned}
\tag{3.48}
$$

$$
\begin{aligned}
v_1(\eta_1,\eta_2,\dot\eta_1,\dot\eta_2) &= \frac{\phi_{1-}}{\beta\phi_1}\left(1-\frac{\phi_{1+}}{\phi_{1-}}\exp(-2\eta_1\frac{\phi_{1-}}{2d})\right)\\
&\quad -\frac{\phi_{2-}}{\beta\phi_2}\left(\exp(-(\eta_1-\eta_2)\frac{\phi_{2+}}{2d})-\frac{\phi_{2+}}{\phi_{2-}}\exp(-(\eta_1+\eta_2)\frac{\phi_{2-}}{2d})\right),
\end{aligned}
\tag{3.49}
$$

$$
\begin{aligned}
v_2(\eta_1,\eta_2,\dot\eta_1,\dot\eta_2) &= \frac{\phi_{2+}}{\beta\phi_2}\left(1+\exp(-2\eta_2\frac{\phi_{2-}}{2d})\right)\\
&\quad -\frac{\phi_{1+}}{\beta\phi_1}\left(\exp(-(\eta_1-\eta_2)\frac{\phi_{1-}}{2d})+\exp(-(\eta_1+\eta_2)\frac{\phi_{1-}}{2d})\right).
\end{aligned}
\tag{3.50}
$$

The derivation of (3.44), (3.45) is stated in Appendix B. If $\dot\eta_i(t)$ is constant, say c and $\eta_1(t)-\eta_2(t)$ is constant with very large $\eta_i(t)$ $(i=1,2)$, say s, then (3.44) and (3.45) reduce to (3.28) and (3.29), respectively. This implies that (3.44)-(3.50) possesses travelling pulse solutions of (3.28),(3.29).

In particular, if $\eta_1(t)$ is very large, (3.44),(3.45) is reduced to a slightly simple form

$$m(\dot{\eta}_1)\ddot{\eta}_1 - \tilde{n}(\eta_1 - \eta_2, \dot{\eta}_2)\ddot{\eta}_2 = 1 - 2a - \tilde{v}_1(\eta_1, \eta_2, \dot{\eta}_1, \dot{\eta}_2) - \frac{\tau\dot{\eta}_1}{\sqrt{(\tau\dot{\eta}_1)^2 + 4}}, \quad t > 0, \tag{3.51}$$

$$m(\eta_2, \dot{\eta}_2)\ddot{\eta}_2 - \tilde{n}(\eta_1 - \eta_2, -\dot{\eta}_1)\ddot{\eta}_1 = -1 + 2a + \tilde{v}_2(\eta_1, \eta_2, \dot{\eta}_1, \dot{\eta}_2) - \frac{\tau\dot{\eta}_2}{\sqrt{(\tau\dot{\eta}_2)^2 + 4}}, \quad t > 0, \tag{3.52}$$

where

$$m(\dot{\eta}_1) = \frac{12d^2}{\phi_1^5}, \tag{3.53}$$

$$\tilde{n}(s,k) = \left(\frac{s^2}{\phi^3(k)} + \frac{6ds}{\phi^4(k)} + \frac{12d^2}{\phi^5(k)}\right)\exp(-s\frac{\phi_+(k)}{2d}) \tag{3.54}$$

with $\phi(k) = \sqrt{k^2 + 4d\beta}$ and $\phi_\pm(k) = \phi(k) \pm k$,

$$\tilde{v}_1(\eta_1, \eta_2, \dot{\eta}_1, \dot{\eta}_2) = \frac{\phi_{1-}}{\beta\phi_1} - \frac{\phi_{2-}}{\beta\phi_2}\exp(-(\eta_1 - \eta_2)\frac{\phi_{2+}}{2d}), \tag{3.55}$$

$$\begin{aligned}\tilde{v}_2(\eta_1, \eta_2, \dot{\eta}_1, \dot{\eta}_2) &= \frac{\phi_{2+}}{\beta\phi_2}\left(1 + \exp(-2\eta_2\frac{\phi_{2-}}{2d})\right) \\ &\quad -\frac{\phi_{1+}}{\beta\phi_1}\exp(-(\eta_1 - \eta_2)\frac{\phi_{1-}}{2d}).\end{aligned} \tag{3.56}$$

We fix τ suitably such that $c(\tau)$ is very small and take the initial conditions as

$$\begin{aligned}&\eta_1(0) = \alpha + s(\tau), \\ &\eta_2(0) = \alpha, \\ &\dot{\eta}_i(0) = -c(\tau)\ (<0)\ \ (i = 1, 2),\end{aligned} \tag{3.57}$$

where α is arbitrarily fixed large. Numerical computation of (3.51), (3.52) clearly shows that the solutions $\eta_i(t)$ $(i = 1, 2)$ exhibit repulsive process as in Figure 3.19, which is qualitatively similar to the one in Figure 3.14.

In order to understand the dynamics of $(\eta_1(t), \eta_2(t))$ of (3.51),(3.52), we classify it into the following 3-stages:

(i) $\eta_1(t) \gg 1$, $\eta_1(t) - \eta_2(t) \gg 1$ and $\dot{\eta_1}(t) < 0$;

(ii) $\eta_1(t) \gg 1$, $\eta_2(t) \gg 1$ and $\eta_1(t) - \eta_2(t) = O(1)$;

(iii) $\eta_1(t) \gg 1, \eta_1(t) - \eta_2(t) \gg 1$ and $\dot{\eta_1}(t) > 0$.

Depending on the stages (i)-(iii), (3.51),(3.52) can be simplified as follows:

Stage (i): Since $\eta_1(t) - \eta_2(t)$ is very large, the interfaces $\eta_1(t)$ and $\eta_2(t)$ are independent, so that (3.51),(3.52) is simply decoupled as

$$m(\dot{\eta_1})\ddot{\eta_1} = 1 - 2a - \hat{v}_1(\dot{\eta_1}) - \frac{\tau\dot{\eta_1}}{\sqrt{(\tau\dot{\eta_1})^2 + 4}}, \tag{3.58}$$

$$m(\eta_2, \dot{\eta_2})\ddot{\eta_2} = -1 + 2a + \hat{v}_2(\eta_2, \dot{\eta_2}) - \frac{\tau\dot{\eta_2}}{\sqrt{(\tau\dot{\eta_2})^2 + 4}}, \tag{3.59}$$

where

$$\hat{v}_1(\dot{\eta_1}) = \frac{\phi_{1-}}{\beta\phi_1}, \tag{3.60}$$

$$\hat{v}_2(\eta_2, \dot{\eta_2}) = \frac{\phi_{2+}}{\beta\phi_2}\left(1 + \exp(-2\eta_2\frac{\phi_{2-}}{2d})\right). \tag{3.61}$$

Putting $\dot{\eta_1} = \xi_1$ into (3.58) leads the equation for ξ_1 as follows:

$$m(\xi_1)\dot{\xi_1} = 1 - 2a - \frac{1}{\beta} + \frac{\xi_1}{\beta\sqrt{\xi_1^2 + 4d\beta}} - \frac{\tau\xi_1}{\sqrt{(\tau\xi_1)^2 + 4}} \equiv S(\xi_1; \tau), \quad t > 0. \tag{3.62}$$

There is the critical value τ_c such that (3.62) has one critical point $\xi_1 = \lambda_1 < 0$ for $\tau_c < \tau$ and three critical points $\xi_1 = \lambda_i$ $(i = 1, 2, 3)$ satisfying $\lambda_1 < 0 < \lambda_2 < \lambda_3$ for $0 < \tau < \tau_c$ where $\xi_1 = \lambda_1, \lambda_3$ are asymptotically stable, while $\xi_1 = \lambda_2$ is unstable (Figures 3.20a and 3.20b). In particular, if $\gamma = \gamma_*$ (or $1 - 2a - 1/\beta = 0$), then $-\lambda_1 = \lambda_3$ and $\lambda_2 = 0$. We fix τ suitably to satisfy $0 < \tau < \tau_c$. One thus finds that the velocity of the interface $\eta_1(t)$ is approximately λ_1. We next consider (3.59). If η_2 is very large, then $\xi_2 = \dot{\eta_2}$ satisfies

$$m(\xi_2)\dot{\xi_2} = -1 + 2a + \frac{1}{\beta} + \frac{\xi_2}{\beta\sqrt{\xi_2^2 + 4d\beta}} - \frac{\tau\xi_2}{\sqrt{(\tau\xi_2)^2 + 4}} \equiv -S(-\xi_2; \tau), \quad t > 0. \tag{3.63}$$

Therefore, the velocity of the interface $\eta_2(t)$ is approximately $-\lambda_3$. If $\eta_2(t)$ approaches the wall $x = 0$, that is, $\eta_2(t) = O(1)$, the dynamics of $\eta_2(t)$ is no longer described by (3.63) but by (3.59). Using phase plane analysis, one finds that if τ is small, the interface $x = \eta_2(t)$ which moves with approximate velocity $-\lambda_3$ hits the wall $x = 0$ (Figure 3.21), while if τ is close to τ_c, it moves very slowly and repels with the wall $x = 0$, and then moves to the left direction where the velocity is asymptotically $-\lambda_1$ (Figure 3.22). Thus, if $\eta_1(t) - \eta_2(t) \gg 1$ is satisfied, $\eta_1(t)$ and $\eta_2(t)$ asymptotically move with velocities λ_1 and $-\lambda_1$, respectively.

Stage (ii): After Stage (i), one finds that $\eta_1(t)$ and $\eta_2(t)$ approach and satisfy $\eta_1(t) - \eta_2(t) = O(1)$. As they are no longer decoupled, we have to consider (3.51),(3.52) simultaneously. Since Stage (i) indicates that $\eta_1(t)$ and $\eta_2(t)$ moves with opposite velocities λ_1 and $-\lambda_1$ after repulsion, we may assume $\dot{\eta_1}(t) = -\dot{\eta_2}(t)$. Therefore, putting $2\eta(t) = \eta_1(t) - \eta_2(t)$ reduces from (3.51), (3.52) to the 2-dimensional ODEs for η only:

$$(m(\dot{\eta}) + \bar{n}(\eta, \dot{\eta}))\ddot{\eta} = 1 - 2a - \bar{v}(\eta, \dot{\eta}) - \frac{\tau\dot{\eta}}{\sqrt{(\tau\dot{\eta})^2 + 4}}, \tag{3.64}$$

$$\bar{n}(\eta, \dot{\eta}) = \left(\frac{4\eta^2}{\phi^3} + \frac{12d\eta}{\phi^4} + \frac{12d^2}{\phi^5}\right)\exp(-2\eta\frac{\phi_{1-}}{2d}), \tag{3.65}$$

$$\bar{v}(\eta, \dot{\eta}) = \frac{\phi_-}{\beta\phi}\left(1 - \frac{\phi_+}{\beta\phi_-}\exp(-2\eta\frac{\phi_-}{2d})\right). \tag{3.66}$$

Using the phase plane analysis in (3.64) again, it is found that $\eta_1(t)$ and $\eta_2(t)$ repel each other with the center $(\eta_1 + \eta_2)/2$ (Figure 3.23).

Stage (iii): Since this stage is treated in a similar way to Stage (i), we omit the discussion.

Consequently, we can understand that the repulsive interaction of very slowly travelling interfaces essentially consists of three stages described by the 2-dimensional ODEs (3.58),(3.59) and (3.64); one is the front-front interaction (Stage (i) and (iii)), the other is the back-back one (Stage (ii)). We should note that the system (3.64) to describe the back-back interaction was already proposed in [15] and if $\eta_1 - \eta_2$ is constant, the pulse-pulse interaction was also studied in [16].

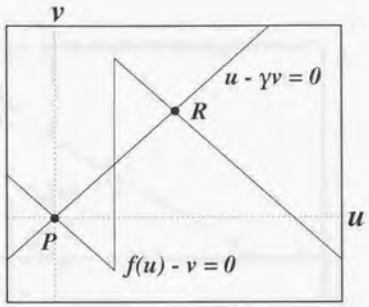

Figure 3.15: Nulclines of f and g of the piecewise-linear nonlinearities in (3.1) where $a = 0.25, \gamma = 0.9999999$.

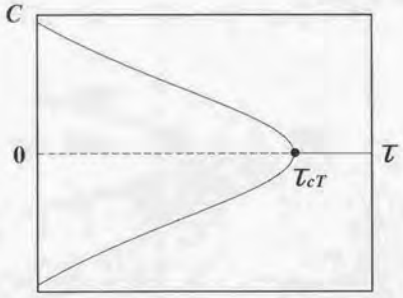

Figure 3.16: Relation between the velocity c and the parameter τ where $d = 1.0, a = 0.25, \gamma = 0.9999999, \tau_{ct} = 0.353554$.

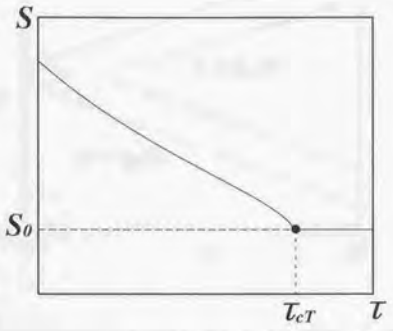

Figure 3.17: Relation between the width s and the parameter τ where the parameters are the same as those in Figure 3.16.

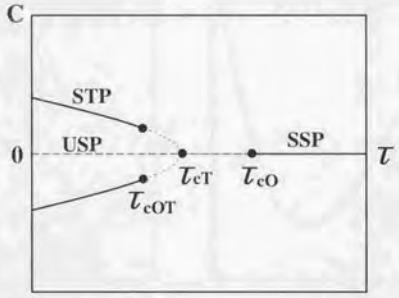

Figure 3.18: Schematic bifurcation diagram of travelling pulses with the parameter τ, where the vertical axis indicates the velocity of the travelling pulse. (SSP: stable standing pulse, USP: unstable standing pulse, STP: stable travelling pulse.)

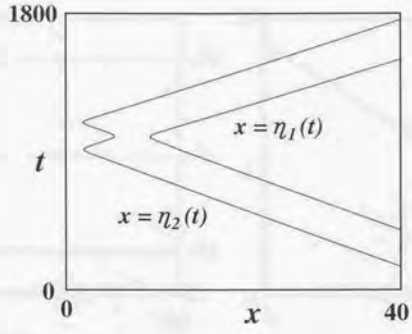

Figure 3.19: Repulsion of the interfaces $\eta_1(t)$ and $\eta_2(t)$ where $d = 1.0, a = 0.25, \gamma = 0.9999999, \tau = 0.3535, c = 0.05669, s = 12.1537$.

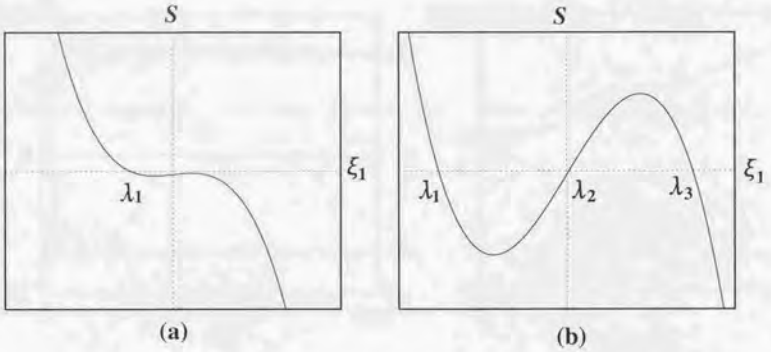

Figure 3.20: Profile of $S(\xi; \tau)$ where $d = 1.0, a = 0.25, \gamma = 0.9999999$: (a) $\tau = 0.35355$; (b) $\tau = 0.3535$.

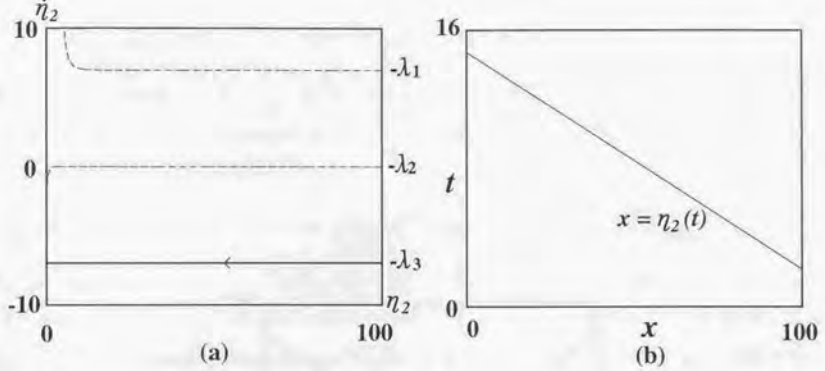

Figure 3.21: Annihilation of the front interface where the parameters are the same as those in Figure 3.19 except $\tau = 0.15$: (a) Trajectory of (3.59) in the $(\eta_2, \dot{\eta}_2)$-plane; (b) Time evolution of $\eta_2(t)$ of (3.59).

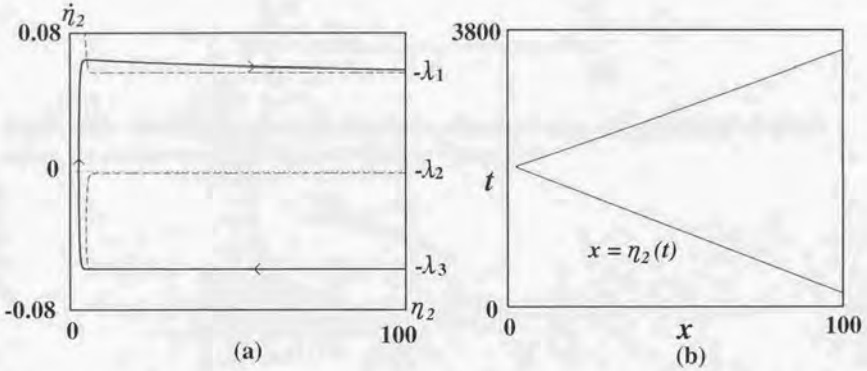

Figure 3.22: Repulsion of the front interface where the parameters are the same as those in Figure 3.19 except $\tau = 0.3535$: (a) Trajectory of (3.59) in the $(\eta_2, \dot{\eta}_2)$-plane; (b) Time evolution of $\eta_2(t)$ of (3.59).

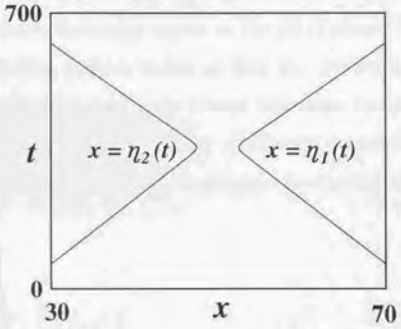

Figure 3.23: Repulsion of the back interfaces. Time evolution of $(\eta_1(t), \eta_2(t))$ of (3.64) where the parameters are the same as those in Figure 3.19.

4 Concluding remarks

4.1 Stability of planar travelling pulses

In the Introduction, we stated in (E-4) that destabilization of planar travelling pulse is one of the feature to generate complex patterns in 2 dimensins. Thus, we consider the following problem for (2.1) which satisfies (A-1) and (A-2):

(Q) *When 1-dimensional travelling pulses are stable, how is their planar stability ?*

Numerical simulations show that the stability of planar travelling pulses depends on values of ε and d. Figure 4.1 shows the stable region in the (d, ε)-plane. Fix ε to be small. If d is small, the planar travelling pulse is stable so that the corresponding ring patterns are also stable. However, when d increases, by lateral inhibition instability, travelling pulses are planarly destabilized (Figure 4.2). Planar oscillating propagating pulses are always unstable so that 2-dimensinal back-firing phenomenon is observed (Figure 4.3).

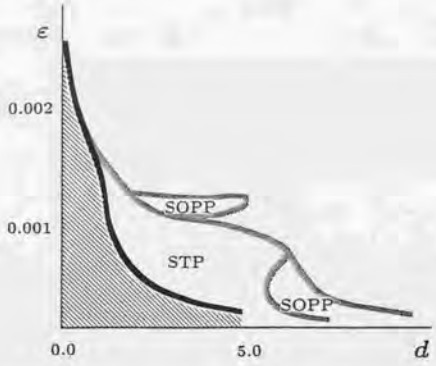

Figure 4.1: Stability of planar travelling pulses in the (ε, d)-plane where the bald curve separates the stable and unstable regions.

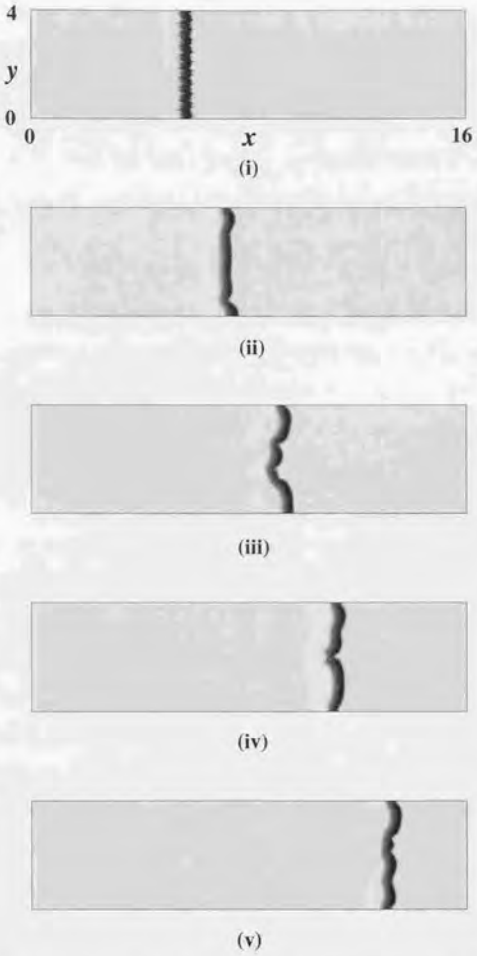

Figure 4.2: Planar instability of a travelling pulse where $\varepsilon = 0.0006, d = 4.5$.

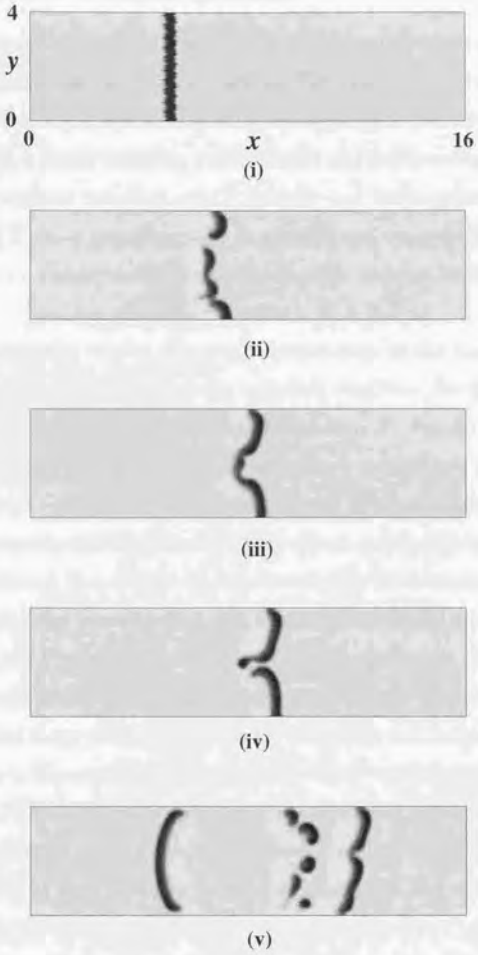

Figure 4.3: Planar instability of an oscillating propagating pulse where $\varepsilon = 0.0012, d = 2.6$.

4.2 Generation of complex patterns

In the previous subsection, we have found that travelling pulses have two features: One is nonannihilation and the other is planar instability. Therefore, taking the parameters ε and d suitably, we find that the characteristics of travelling pulses is basically classified into the following 4 cases: (i) a planar travelling pulse is stable and two travelling pulses annihilate upon collision; (ii) a planar travelling pulse is unstable and two travelling pulses annihilate upon collision; (iii) a planar travelling pulse is unstable and two travelling pulses fade out before collision; (iv) a planar travelling pulse is unstable and two travelling pulses reflect before collision.

Consider the dynamics of ring patterns corresponding to the cases (i)-(iv) in a 2-dimensional square domain with the zero-flux boundary condition. For the initial condition, we take a droplet disturbance of u to the equilibrium state P. For the case (i), one could easily expect that an expanding ring collides and simply annihilates, as shown in Figure 1.8. For the case (ii), a ring pattern always expands with circular shape (Figure 4.4), which seems to be similar to the case (i), but, when the radius is sufficiently large, the ring might be destabilized, although it could not be demonstrated by our computation. However, if spiral waves are generated in a standard way, they are destabilized and breaks down into complex pattern, as in Figure 4.5. For the case (iii), a ring pattern is clearly deformed and finally comes to small pieces, because of the reflection boundary (Figure 4.6). For the case (iv), the destabilized rings autonomously breaks down into many irregular spots(Figure 4.7). We can observe three types of the interaction of two expanding rings, depending on the size of radius. When the size is large, two rings approach, reflect and then break up into several pieces (Figure 4.8a), while when the size is middle, two rings approach closely and the nearest parts of them gradually fade out (Figure 4.8b), and when the size is small, two rings approach and annihilate each other (Figure 4.8c). These properties help us to understand why expanding rings are broken into many small spots. In this situation, if the initial distribution is exactly the same as the one in Figure 4.5, it no longer generate spiral

waves but produces small spots from the tip (Figure 4.9). Breakup of spiral patterns is also discussed in bistable RD systems [3, 4].

In order to confirm that complex patterns occur due to two effects of nonannihilation property and planar instability and these are generated if there exist very slowly travelling pulses, we consider again the Gray-Scott model (2.2) with $p(u) = u^2$. When travelling pulses have very slow velocity, planar travelling pulses is unstable as shown in Figure 4.10. This phenomena are also observed in (2.2) with $p(u) = \exp(u)$. Therefore, we arrived at the following conjecture:

(C-2) If very slowly travelling pulses exist, then planar travelling pulses are unstable.

Moreover, an expanding ring was broken down into complex spot pattern by nonannihilation property and planar instability. This is shown in Figure 4.11, which is similar to the one in Figure 4.7. Therefore, we obtain the following conjecture:

The mechanism generating complex pattern in RD systems (1.1) with excitability is the existence of very slowly travelling pulses.

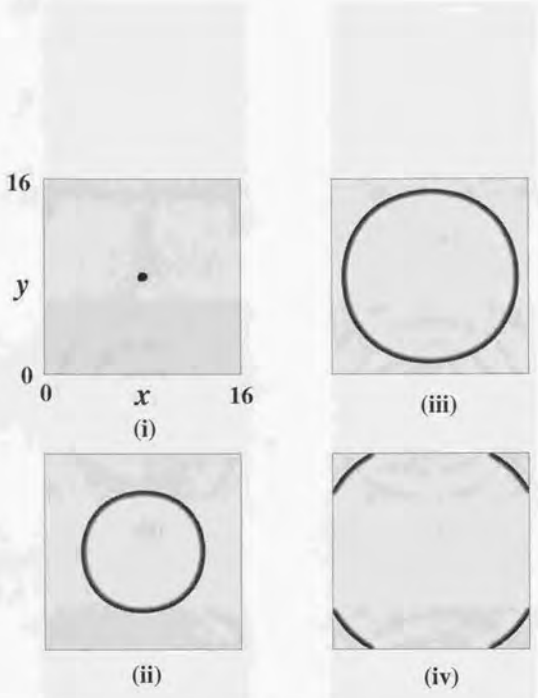

Figure 4.4: Annihilation of expanding rings where $\varepsilon = 0.00045, d = 4.5$.

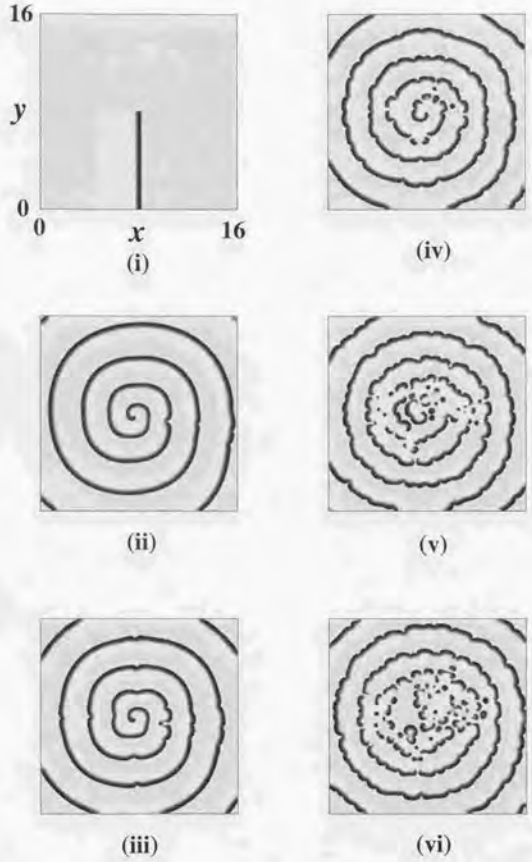

Figure 4.5: Breakdown of spiral pattern where the parameters are the same as the ones in Figure 4.4.

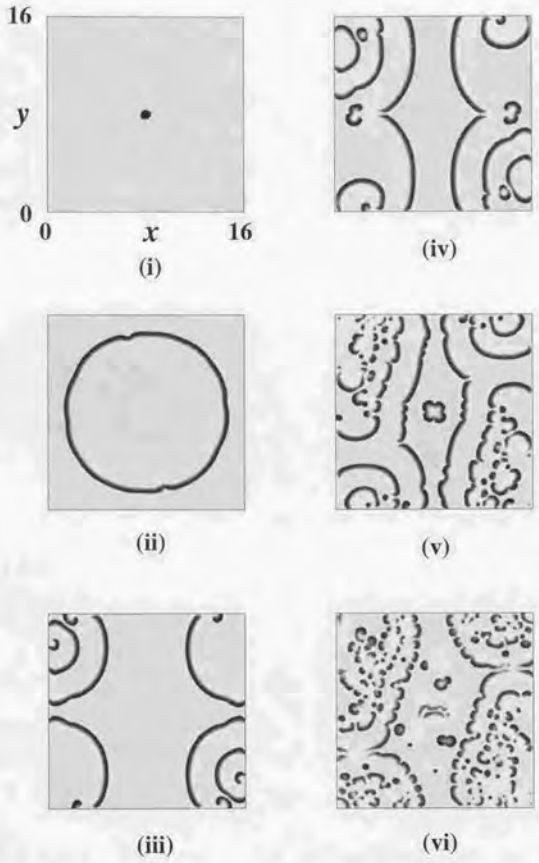

Figure 4.6: Deformed expanding ring where $\varepsilon = 0.00065, d = 4.5$.

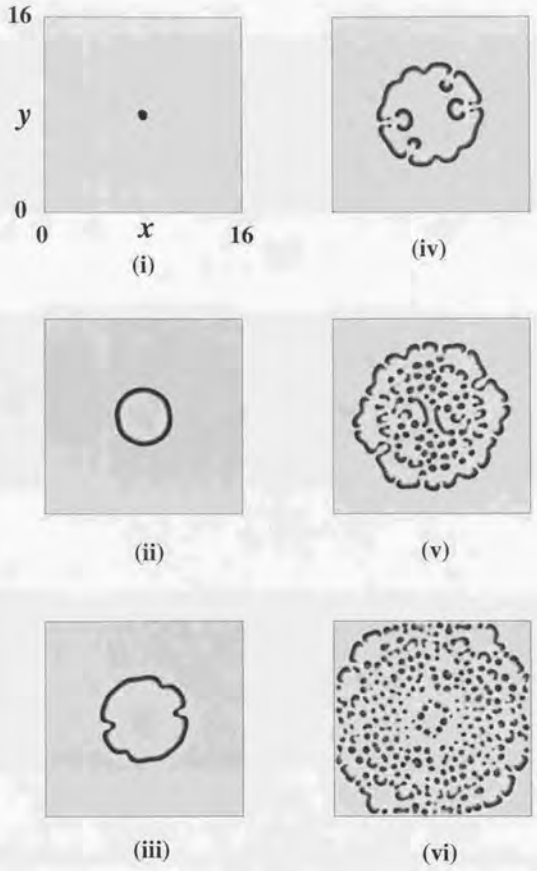

Figure 4.7: Breakdown of one expanding ring where $\varepsilon = 0.001, d = 4.5$.

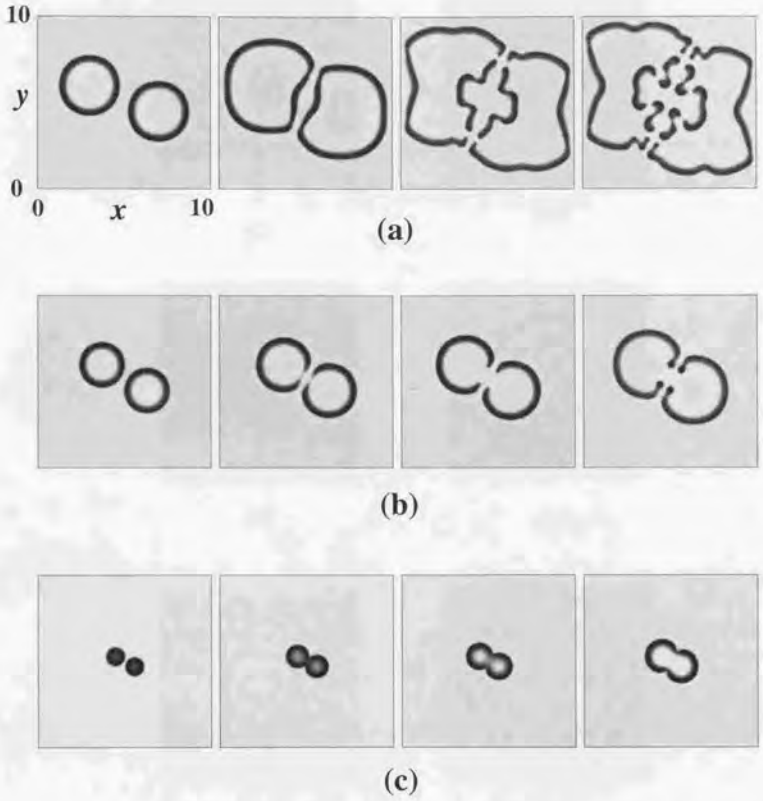

Figure 4.8: Collision of two expanding rings where the parameters are the same as the ones in Figure 4.7: (a) Large size rings; (b) Middle size rings; (C) Small size rings.

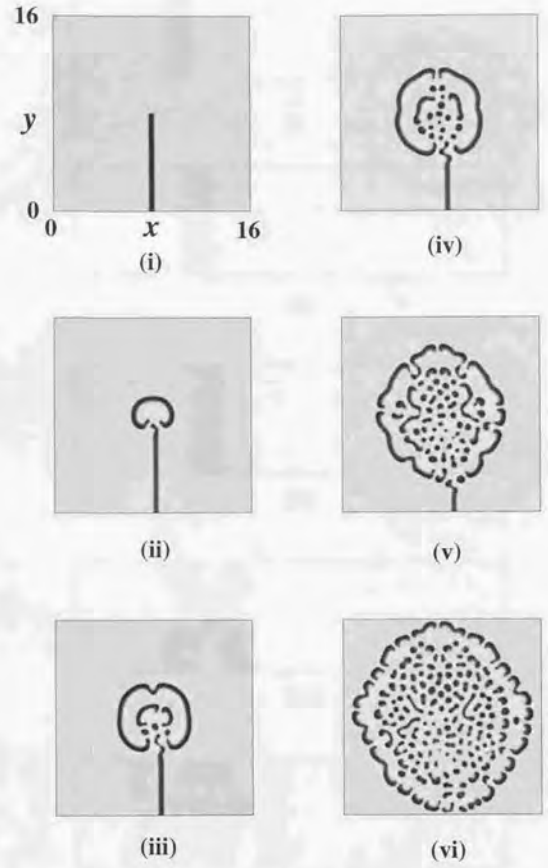

Figure 4.9: Breakdown into spot patterns where the parameters are the same as the ones in Figure 4.7.

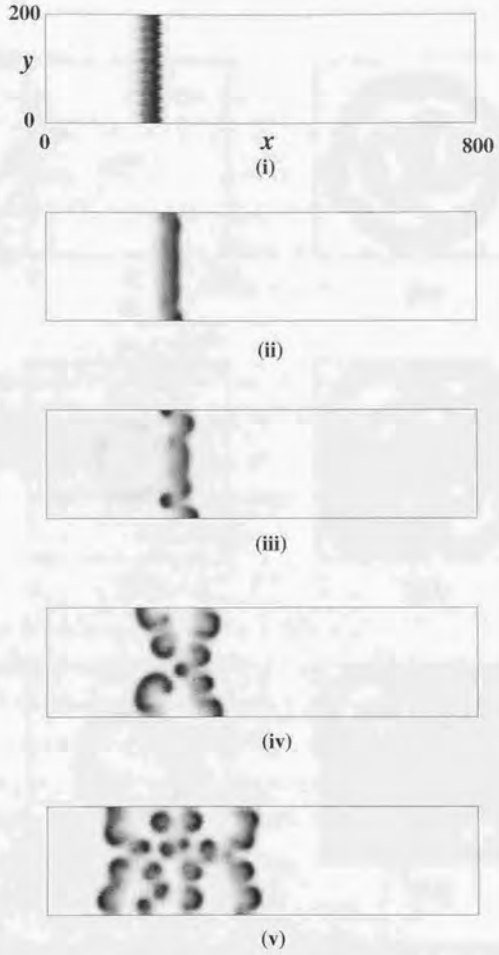

Figure 4.10: Planar instability of travelling pulse of (2.2) where $a = 0.07, h = 0.018, v_c = 1.0, \varepsilon = 1.0, d = 3.5$.

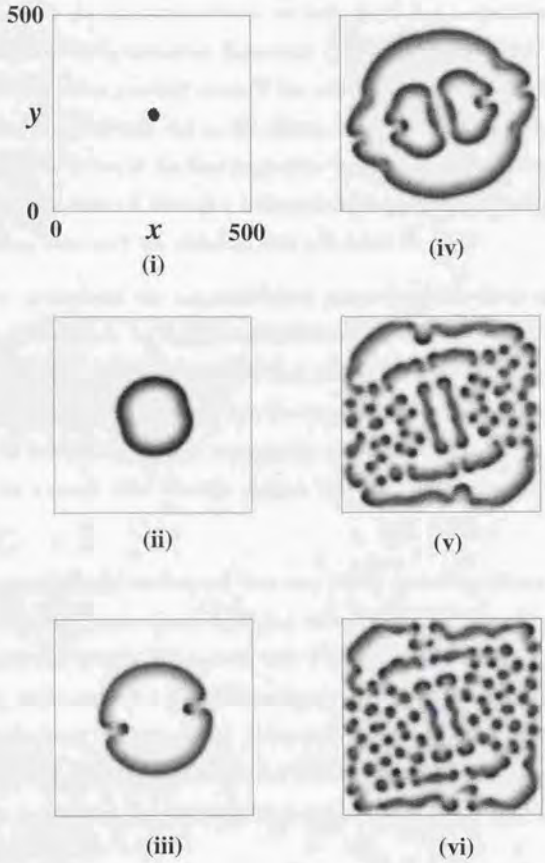

Figure 4.11: Breakdown of one expanding ring where the parameters are the same as the ones in Figure 4.10.

4.3 Summary

By the discussions in the previous sections, we have given two conjectures by using analytical and complementarily numerical discussion: (1) Nonannihilation and planar destabilization of travelling pulses possibly occur, if the velocity is very slow; (2) Spatio-temporal complex patterns are generated due to the effects of nonannihilation and planar destabilization. We therefore arrive at the final conjecture that 2-dimensional complex patterns in excitable RD systems occur, if there is a 1-dimensional very slowly travelling pulses. More precisely speaking, the result has obtained here are stated in order:

(1) In order to understand the nonannihilation property of travelling pulses arising in excitable RD system, we have investigated an exothermic RD system (2.1). By numerical computation, we have found that the essence of nonannihilation property of travelling pulse is the existence of very slowly travelling pulses with lateral inhibition. In order to confirm it, we have numerically shown that its holds for the Gray-Scott model. As a result, this strongly suggest that its holds for any 2-component RD systems.

(2) In order to analytically understand that very slowly travelling pulses with lateral inhibition approach each other, repel and move in the opposite direction, we have investigated the bistable RD system with FHN nonlinearities. Using the interfacial approach, we have derived the 4-dimensional ODEs to describe the very slow motion of interfaces from the RD system. Although the derivation is formal and has not yet been justified, it has confirmed that the reduced ODEs is a good approximated system to understand the repulsive interaction of very slowly travelling pulses with lateral inhibition.

(3) In order to understand the mechanism generating complex pattern as Fig.1.10, we have investigated an exothermic RD system (2.1) by numerical computation. As a result, we have found that complex patterns are generated by nonannihilation and

planar instability of travelling pulses and if very slowly travelling pulses with lateral inhibition exist, planar travelling pulses are unstable. In order to confirm it, we have investigated for the Gray-Scott model. Then we have obtained the same result as an exothermic RD system. Therefore, we have obtained the conjecture that the mechanism generating complex pattern is the existence of very slowly travelling pulses with lateral inhibition.

5 Appendix

5.1 Appendix A

Taking the limit $\varepsilon \downarrow 0$ in (3.1), we derive the evolutional equation for two interfacial points $\eta_F(t)$ and $\eta_B(t)$ satisfying $0 < \eta_F(t) < \eta_B(t)$, in $\boldsymbol{R}$. We formally put $\varepsilon = 0$ in (3.1) and then obtain

$$v = f(u), \tag{A.1}$$

$$\frac{\partial v}{\partial t} = d\frac{\partial^2 v}{\partial x^2} + \begin{cases} h_-(v) - \gamma v, & t > 0, \quad x \in \boldsymbol{R} \setminus (\eta_F(t), \eta_B(t)), \\ h_+(v) - \gamma v, & t > 0, \quad x \in (\eta_F(t), \eta_B(t)), \end{cases} \tag{A.2}$$

To determine the motion of the interface $x = \eta_B(t)$, for instance, let us introduce the new variable ξ instead of x

$$\xi = \frac{x - \eta_B(t)}{\varepsilon}, \quad | x - \eta_B(t) | < \delta, \tag{A.3}$$

where $\delta = O(1)$. The resulting equations from (3.1) are given by

$$-\tau\dot{\eta_B}(t)\tilde{u}_\xi + \tau\varepsilon\tilde{u}_t = \tilde{u}_{\xi\xi} + f(\tilde{u}) - \tilde{v}, \tag{A.4}$$

$$t > 0, \quad -\delta/\varepsilon < \xi < \delta/\varepsilon,$$

$$-\varepsilon\dot{\eta_B}(t)\tilde{v}_\xi + \varepsilon^2\tilde{v}_t = d\tilde{v}_{\xi\xi} + \varepsilon^2(\tilde{u} - \gamma\tilde{v}), \tag{A.5}$$

where $\tilde{u}(t,\xi) = u(t,\eta_B(t)+\varepsilon\xi), \tilde{v}(t,\xi) = v(t,\eta_B(t)+\varepsilon\xi)$. In the limit $\varepsilon \downarrow 0$, (A.4),(A.5) formally become

$$-\tau\dot{\eta_B}(t)\tilde{u}_\xi = \tilde{u}_{\xi\xi} + f(\tilde{u}) - \tilde{v}, \tag{A.6}$$

$$t > 0, \quad -\infty < \xi < +\infty,$$

$$d\tilde{v}_{\xi\xi} = 0, \tag{A.7}$$

where the boundary conditions are

$$\tilde{u}(t,\pm\infty) = h_\mp(v(t,\eta_B(t))), \tag{A.8}$$

$$\tilde{v}(t,\pm\infty) = v(t,\eta_B(t)). \tag{A.9}$$

From (A.7) and (A.9), we obtain

$$\tilde{v}(t,\xi) = v(t,\eta_B(t)) \quad \text{for any } \xi \in \boldsymbol{R}. \tag{A.10}$$

Therefore, (A.5) reduces to the following scalar equation for $\tilde{u}$ with the parameter t:

$$-\tau\dot{\eta_B}(t)\tilde{u}_\xi = \tilde{u}_{\xi\xi} + f(\tilde{u}) - v(t,\eta_B(t)), \tag{A.11}$$

$$\tilde{u}(t,\pm\infty) = h_\mp(v(t,\eta_B(t))). \tag{A.12}$$

Solving the following nonlinear eigenvalue problem with λ

$$\begin{cases} -\lambda u_z = u_{zz} + f(u) - \xi, & z \in \boldsymbol{R}, \\ u(+\infty) = h_-(\xi), \quad u(-\infty) = h_+(\xi), \end{cases} \tag{A.13}$$

we obtain the interface equation for $\eta_B(t)$ as

$$\tau\dot{\eta_B}(t) = \lambda(v(t,\eta_B(t))). \tag{A.14}$$

By using the similar argument to the above, the interface equation for $\eta_F(t)$ is also given by

$$\tau\dot{\eta_F}(t) = -\lambda(v(t,\eta_F(t))). \tag{A.15}$$

5.2 Appendix B

We derive the interface equations (3.44),(3.45). We extend $\boldsymbol{R}_+$ to the whole domain $\boldsymbol{R}$, by using the mirror symmetry at $x = 0$. Applying the Fourier transform given by

$$v_q(t) = \int_{-\infty}^{\infty} v(x,t)e^{iqx}dx$$

to (3.38), we have

$$\dot{v_q}(t) = -(dq^2 + \beta)v_q(t) + \frac{2}{q}(\sin(q\eta_1(t)) - \sin(q\eta_2(t)), \tag{B.1}$$

where the term $v_q(0)\exp(-(dq^2 + \beta)t)$ was ignored, since we consider the dynamics after large time. The inverse Fourier transform of (B.1) yields

$$\begin{aligned} v(t,x) &= \frac{1}{2\pi}\int_{-\infty}^{\infty}\frac{2}{q}\int_0^t \exp(-(dq^2+\beta)(t-s) - iqx)\sin(q\eta_1(s))ds\ dq \\ &\quad -\frac{1}{2\pi}\int_{-\infty}^{\infty}\frac{2}{q}\int_0^t \exp(-(dq^2+\beta)(t-s) - iqx)\sin(q\eta_2(s))ds\ dq. \end{aligned} \tag{B.2}$$

Hence we obtain

$$\begin{aligned} v_1(t) &= v(t,\eta_1(t)) \\ &= \frac{1}{2\pi}\int_{-\infty}^{\infty}\frac{2}{q}\int_0^t \exp(-(dq^2+\beta)(t-s) - iq\eta_1(t))\sin(q\eta_1(s))ds\ dq \\ &\quad -\frac{1}{2\pi}\int_{-\infty}^{\infty}\frac{2}{q}\int_0^t \exp(-(dq^2+\beta)(t-s) - iq\eta_1(t))\sin(q\eta_2(s))ds\ dq \end{aligned} \tag{B.3}$$

and

$$\begin{aligned} v_2(t) &= v(t,\eta_2(t)) \\ &= \frac{1}{2\pi}\int_{-\infty}^{\infty}\frac{2}{q}\int_0^t \exp(-(dq^2+\beta)(t-s) - iq\eta_2(t))\sin(q\eta_1(s))ds\ dq \\ &\quad -\frac{1}{2\pi}\int_{-\infty}^{\infty}\frac{2}{q}\int_0^t \exp(-(dq^2+\beta)(t-s) - iq\eta_2(t))\sin(q\eta_2(s))ds\ dq. \end{aligned} \tag{B.4}$$

(B.3) and (B.4) indicate that there is a time-delayed interaction between two pulses mediated by v. Therefore, to solve (B.3) and (B.4), we take account of the effects of the

time-delayed interaction perturbatively and employ the following approximation:

$$\eta_i(s) = \eta_i(t) + \dot{\eta}_i(t)(s-t) + \ddot{\eta}_i(t)\frac{(s-t)^2}{2} + \cdots \quad (i = 1, 2). \tag{B.5}$$

More precise explanation of (B.5) is stated in Appendix C. After straightforward calculation, we approximate (B.3) up to $O(\ddot{\eta}_i)$ as

$$v_1(t) = v_1^{(1)}(t) + v_1^{(2)}(t), \tag{B.6}$$

where the term of $O(e^{-\beta t})$ was ignored, since we consider the dynamics after large time and

$$\begin{aligned} v_1^{(1)}(t) &= \frac{1}{2\pi}\int_{-\infty}^{\infty}\frac{2}{2iq}\left(\frac{1}{dq^2+\beta+iq\dot{\eta}_1} - \frac{\exp(-2iq\eta_1)}{dq^2+\beta-iq\dot{\eta}_1}\right. \\ &\quad \left. -\frac{\exp(-iq(\eta_1-\eta_2))}{dq^2+\beta+iq\dot{\eta}_2} + \frac{\exp(-iq(\eta_1+\eta_2))}{dq^2+\beta-iq\dot{\eta}_2}\right)dq \\ &= \frac{1}{2\beta\phi_1}\left((\phi_{1-} - \phi_{1+}\exp(-2\eta_1\frac{\phi_{1-}}{2d})\right) \\ &\quad -\frac{1}{2\beta\phi_2}\left(\phi_{2-}\exp(-(\eta_1-\eta_2)\frac{\phi_{2+}}{2d})\right. \\ &\quad \left. -\phi_{2+}\exp(-(\eta_1+\eta_2)\frac{\phi_{2-}}{2d})\right). \end{aligned} \tag{B.7}$$

By (B.3), the first order correction $v_1^{(2)}$ is given as

$$\begin{aligned} v_1^{(2)}(t) &= \frac{1}{2\pi}\int_{-\infty}^{\infty}\ddot{\eta}_1\left(\frac{1}{(dq^2+\beta+iq\dot{\eta}_1)^3} + \frac{\exp(-2iq\eta_1)}{(dq^2+\beta-iq\dot{\eta}_1)^3}\right) \\ &\quad -\ddot{\eta}_2\left(\frac{\exp(-iq(\eta_1-\eta_2))}{(dq^2+\beta+iq\dot{\eta}_2)^3} + \frac{\exp(-iq(\eta_1+\eta_2))}{(dq^2+\beta-iq\dot{\eta}_2)^3}\right)dq. \end{aligned} \tag{B.8}$$

We may derive the equation for v_2 in the similar way to (B.7) so that $v_2^{(1)}$ is given as

$$\begin{aligned} v_2^{(1)}(t) &= \frac{1}{2\pi}\int_{-\infty}^{\infty}\frac{2}{2iq}\Big(-\frac{1}{dq^2+\beta+iq\dot{\eta}_2}+\frac{\exp(-2iq\eta_2)}{dq^2+\beta-iq\dot{\eta}_2} \\ &\quad +\frac{\exp(iq(\eta_1-\eta_2))}{dq^2+\beta+iq\dot{\eta}_1}-\frac{\exp(-iq(\eta_1+\eta_2))}{dq^2+\beta-iq\dot{\eta}_1}\Big)dq \\ &= \frac{1}{2\beta\phi_2}\Big(\phi_{2+}+\phi_{2+}\exp(-2\eta_2\frac{\phi_{2-}}{2d})\Big) \qquad \text{(B.9)} \\ &\quad -\frac{1}{2\beta\phi_1}\Big(\phi_{1+}\exp(-(\eta_1-\eta_2)\frac{\phi_{1-}}{2d}) \\ &\quad +\phi_{1+}\exp(-(\eta_1+\eta_2)\frac{\phi_{-1}}{2d})\Big). \end{aligned}$$

By (B.4), the correction $v_2^{(2)}$ is obtained as

$$\begin{aligned} -v_2^{(2)}(t) &= \frac{1}{2\pi}\int_{-\infty}^{\infty}\ddot{\eta}_2\Big(\frac{1}{(dq^2+\beta+iq\dot{\eta}_2)^3}+\frac{\exp(-2iq\eta_2)}{(dq^2+\beta-iq\dot{\eta}_2)^3}\Big) \qquad \text{(B.10)} \\ &\quad -\ddot{\eta}_1\Big(\frac{\exp(iq(\eta_1-\eta_2))}{(dq^2+\beta+iq\dot{\eta}_1)^3}+\frac{\exp(-iq(\eta_1+\eta_2))}{(dq^2+\beta-iq\dot{\eta}_1)^3}\Big)dq. \end{aligned}$$

Thus one may write $v_1^{(2)}$ and $v_2^{(2)}$ as

$$v_1^{(2)} = m(\eta_1,\dot{\eta}_1)\ddot{\eta}_1 - n_1(\eta_1,\eta_2,\dot{\eta}_2)\ddot{\eta}_2 \qquad \text{(B.11)}$$

and

$$-v_2^{(2)} = m(\eta_2,\dot{\eta}_2)\ddot{\eta}_2 - n_2(\eta_1,\eta_2,\dot{\eta}_1)\ddot{\eta}_1, \qquad \text{(B.12)}$$

where $m(\eta_i,\dot{\eta}_i)$ $(i=1,2)$ are defined by

$$\begin{aligned} m(\eta_i,\dot{\eta}_i) &= \frac{1}{2\pi}\int_{-\infty}^{\infty}\Big(\frac{1}{(dq^2+\beta+iq\dot{\eta}_i)^3}+\frac{\exp(-2iq\eta_i)}{(dq^2+\beta-iq\dot{\eta}_i)^3}\Big)dq \\ &= \frac{6d^2}{\phi_i^{5/2}}(1+\exp(-2\eta_i\phi_{i-})) \qquad \text{(B.13)} \\ &\quad +\Big(\frac{2\eta_i^2}{\phi_i^{3/2}}+\frac{6d\eta_i}{\phi_i^2}\Big)\exp(-2\eta_i\phi_{i-}) \quad (i=1,2). \end{aligned}$$

In the similar way to (B.12), n_1 and n_2 are defined by

$$
\begin{aligned}
n_1 &= \frac{1}{2\pi}\int_{-\infty}^{\infty}\left(\frac{\exp(-iq(\eta_1-\eta_2))}{(dq^2+\beta+iq\dot{\eta}_2)^3}+\frac{\exp(-iq(\eta_1+\eta_2))}{(dq^2+\beta-iq\dot{\eta}_2)^3}\right)dq \\
&= \left(\frac{(\eta_1-\eta_2)^2}{2\phi_2^3}+\frac{3d(\eta_1-\eta_2)}{\phi_2^4}+\frac{6d^2}{\phi_2^5}\right)\exp(-(\eta_1-\eta_2)\phi_{2+}) \qquad \text{(B.14)} \\
&\quad +\left(\frac{(\eta_1+\eta_2)^2}{2\phi_2^3}+\frac{3d(\eta_1+\eta_2)}{\phi_2^4}+\frac{6d^2}{\phi_2^5}\right)\exp(-(\eta_1+\eta_2)\phi_{2-}),
\end{aligned}
$$

$$
\begin{aligned}
n_2 &= \frac{1}{2\pi}\int_{-\infty}^{\infty}\left(\frac{\exp(iq(\eta_1-\eta_2))}{(dq^2+\beta+iq\dot{\eta}_1)^3}+\frac{\exp(-iq(\eta_1+\eta_2))}{(dq^2+\beta-iq\dot{\eta}_1)^3}\right)dq \\
&= \left(\frac{(\eta_1-\eta_2)^2}{2\phi_1^3}+\frac{3d(\eta_1-\eta_2)}{\phi_1^4}+\frac{6d^2}{\phi_1^5}\right)\exp(-(\eta_1-\eta_2)\phi_{1-}) \qquad \text{(B.15)} \\
&\quad +\left(\frac{(\eta_1+\eta_2)^2}{2\phi_1^3}+\frac{3d(\eta_1+\eta_2)}{\phi_1^4}+\frac{6d^2}{\phi_1^5}\right)\exp(-(\eta_1+\eta_2)\phi_{1-}).
\end{aligned}
$$

Therefore (3.44) and (3.45) can be obtained.

5.3 Appendix C

In this section we examine the condition that the approximation (3.43) holds. On the physical ground, the short time expansion for $\eta_1(t)$ and $\eta_2(t)$ is justified. If the characteristic time of a pulse is sufficiently large compared with that of v_1 and v_2. Hereafter we omit the subscript 1 and 2 for η and v, since this distinction is not important in the following argument. (B.3) and (B.4) indicate that $1/\beta$ is the relaxation time of v and that the characteristic length associated with v is $\ell = \sqrt{d/\beta}$. This is the width of the domain tail around a pulse where v is finite. The time necessary for a pulse to propagate at this distance is given by ℓ/c. Therefore the smallness parameter is expected to be $c/(\beta\ell) = c/\sqrt{\beta d}$.

The above fact is directly verified if we introduce the dimensionless variables for η and time t such that $\hat{\eta} = \eta/\ell$ and $\hat{t} = ct/\ell$. Note that (B.3) and (B.4) contain only d and β as parameters and that v has a dimension of time. Therefore v must have the following

scaling form in the short time expansion:

$$v = \frac{1}{\beta} g\left(\beta^{-(m+n)}\ell^{-(n+1)}\frac{d^m\eta}{dt^m}(\frac{d\eta}{dt})^n\right), \tag{C.1}$$

where m and n are positive integers and $g(x)$ is a dimensionless function. In terms of $\hat{\eta}$ and $\hat{t}$, we have

$$\beta^{-(m+n)}\ell^{-(n+1)}\frac{d^m\eta}{dt^m}(\frac{d\eta}{dt})^n = (\frac{c}{\beta\ell})^{n+m}\frac{d^m\hat{\eta}}{d\hat{t}^m}(\frac{d\hat{\eta}}{d\hat{t}})^n. \tag{C.2}$$

This clearly indicates that $c/(\beta\ell)$ is the smallness parameter. This fact has a simple physical interpretation. That is, the short time expansion is justified if the propagating velocity c of a pulse is much smaller than the diffusion "velocity" $\sqrt{\beta d}$ of v. Finally it should be noted that the argument presented here can be applied to both pulse and interface dynamics.

References

[1] M.Bar, M.Hildebrand, M.Eiswirth, M.Falcke, H.Engel and M.Neufeld, *Chemical turbulence and standing waves in a surface reaction model: The influence of global coupling and wave instabilities*, Chaos, **4**(3), 499–508 (1994).

[2] P.Gray and S.K.Scott, *Autocatalytic reaction in the isothermal continuous stirred tank reactor*, Chem. Engng. Sci. bf39, 1087–1097 (1984).

[3] A.Hagberg and E.Meron, *Front labyrinthine patterns to spiral turbulence*, Phys. Rev. Lett. **72**. 2494–2497 (1994).

[4] A.Hagberg and E.Meron, *Complex pattern in reaction-diffusion systems; A tale of tow front instabilities*, Chaos, **4**(3), 477–484 (1994).

[5] D.Hilhost, Y.Nishiura and M.Mimura, *A free boundary problem arising in some reacting-diffusing system*, Proc. Roy. Soc. Edinburgh, **118A**, 1991, 355–378.

[6] H.Ikeda, *Existence and stability of pulse waves bifurcated from front and back waves in bistable reaction-diffusion systems*, to appear in Japan J. Indust. Appl. Math.

[7] T.Ikeda, H.Ikeda and M.Mimura, *Hopf bifurcation of travelling pulses in some bistable reaction-diffusion systems*, manuscript.

[8] S.Kawaguchi and M.Mimura, *Collision of travelling waves in a reaction-diffusion system with global coupling effect*, to appear in SIAM J. Appl. Math. 1997.

[9] K.Krisher and A.Mikhailov, *Bifurcation to travelling spots in reaction-diffusion systems*, Phys. Rev. Lett. **73**, 1994, 3165–3168.

[10] M.Mimura and M.Nagayama, *Nonannihilation dynamics in an exothermic reaction-diffusion system with mono-stable excitability*, to appear in CHAOS, 1997.

[11] M.Mimura, M.Nagayama and T.Ohta, *Nonannihilation of travelling pulses in reaction-diffusion systems*, manuscript.

[12] M.Mimura, M.Nagayama, and K.Sakamoto, *Pattern dynamics in an exothermic reaction*, Physica D **84**, 58–71 (1995).

[13] J.Nagumo, S.Arimoto and S.Yoshizawa, *An active pulse transmission line simulating nerve axon*, Proc. I. R. E. **50**, 1962, 2061–2070.

[14] Y.Nishiura and M.Mimura, *Layer oscillations in reaction-diffusion systems*, SIAM J. Appl. Math.**49**, 1989, 481-514.

[15] T.Ohta and J.Kiyose, *Collison of domain boundaries in a reaction-diffusion system*, J. Phys. Soc. Jpn. **65**, 1996, 1967–1970.

[16] T.Ohta, J.Kiyose and M.Mimura, *Collision of propagating pulse in a reaction-diffusion system*, J. Phys. Soc. Jpn. **66**, 1997, 1551–1558.

[17] J.Pearson, *Complex patterns in a simple system*, Sciences **261**, 1993, 189–192.

[18] V.Petrov, S.K.Scott AND K.Showalter, *Excitability, wave reflection, and wave splitting in a cubic autocatalysis reaction-diffusion systems*, Phil. Trans. R. Sco. Lond. **A347**, 1994, 631–642.

[19] J.Rinzel and D.Terman, *Propagation phenomena in a bistable reaction-diffusion system*, SIAM J. Appl. Math. **42**, 1982, 1111–1137.

[20] T.Tsujikawa, T.Nagai, M.Mimura, R.Kobayashi and H.Ikeda *Stability properties of travelling pulse solutions of the higher dimensional FitzHugh-Nagumo equations*, Japan J. Appl. Math. **6**, 341–366 (1989).

[21] J.J.Tyson and P.C.Fife, *Target patterns in a realistic model of the Belousov-Zhabotinskii reaction*, J. Chem. Phys. **73**(5), 1980. 2224-2237.

[22] A.T.Winfree, in *Theoretical Chemistry Vol.4*, edited by Eyring and D.Henderson, (Academic, New York, 1978), 1-51.

[23] X-F.Chen, *Generation and propagation of interfaces in reaction-diffusion systems*, Trans. Math. Soc. **334**, 1992, 877-913

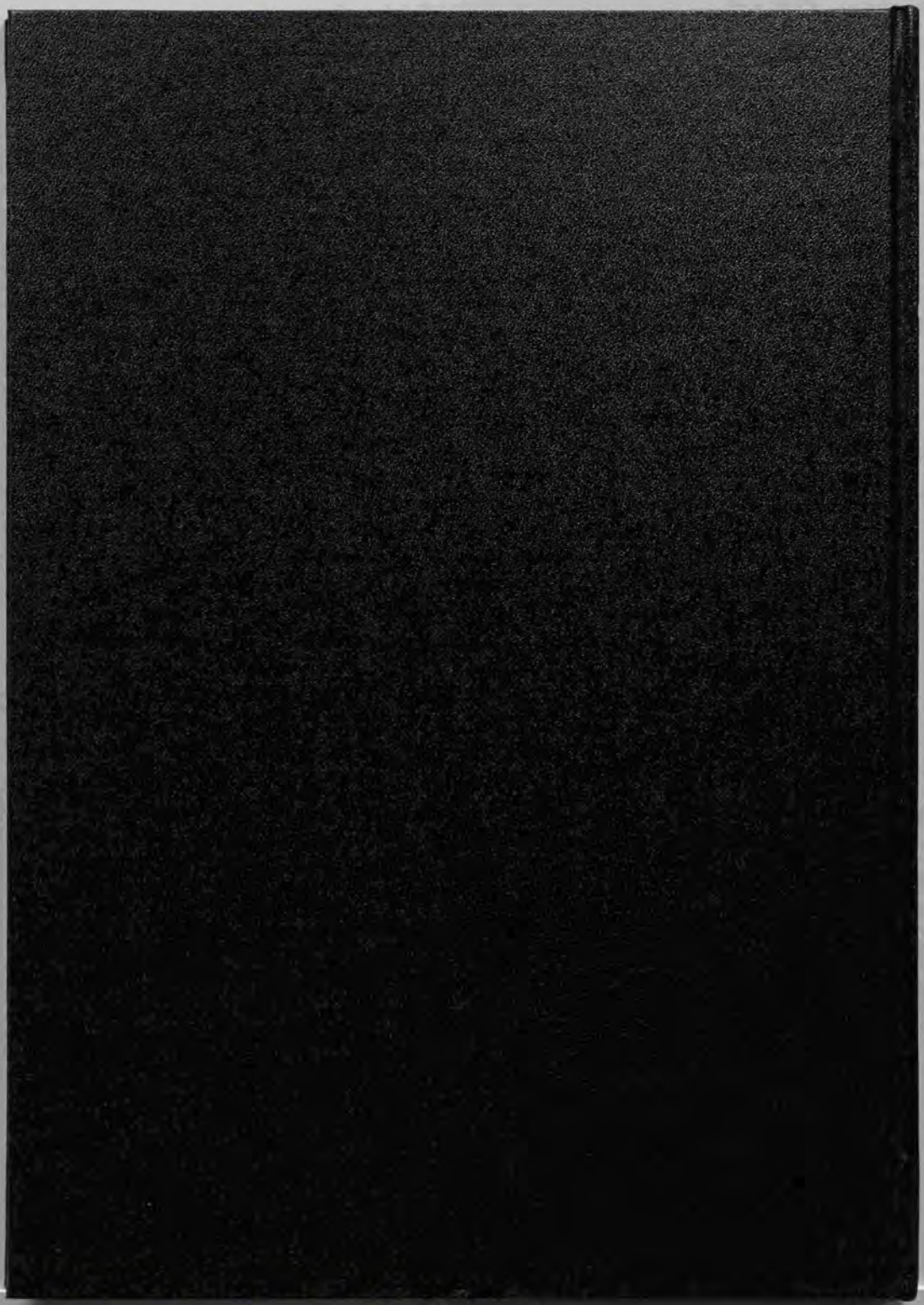

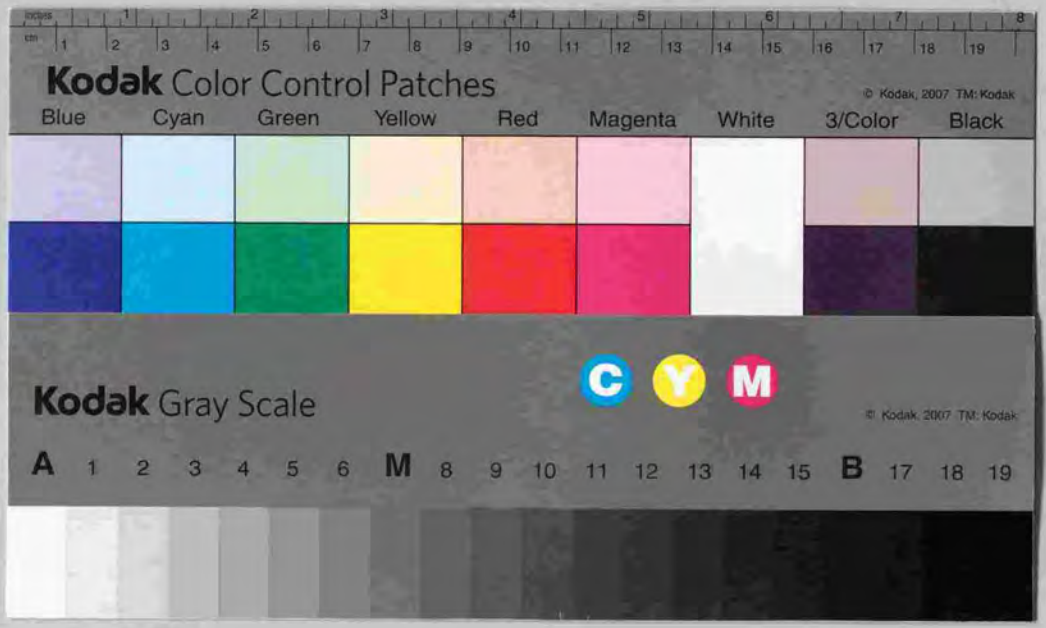
Kodak Color Control Patches
© Kodak, 2007 TM: Kodak
Blue
Cyan
Green
Yellow
Red
Magenta
White
3/Color
Black
Kodak Gray Scale
C
Y
M
© Kodak, 2007 TM: Kodak
A 1 2 3 4 5 6 M 8 9 10 11 12 13 14 15 B 17 18 19